Pacific Community
Communauté du Pacifique

# Assessment of ridge-to-reef management actions in Tagabe watershed and Mele Bay, Vanuatu

gef
UNDP Empowered lives. Resilient nations
FAO FIAT PANIS
UN environment programme
Pacific R2R Ridge to Reef

# Assessment of ridge-to-reef management actions in Tagabe watershed and Mele Bay, Vanuatu

By Dr Jade M.S Delevaux & Dr Kostantinos A Stamoulis

Prepared for the Pacific Ridge to Reef Programme,
Geoscience, Energy and Maritime Division,
Pacific Community (SPC), Suva, Fiji

Pacific Community
Communauté du Pacifique

Suva, Fiji, 2021

Original text: English

Pacific Community Cataloguing-in-publication data

Delevaux, J.M.S

Assessment of ridge-to-reef management actions in Tagabe watershed and Mele Bay, Vanuatu / by Dr Jade M.S Delevaux and Dr Kostantinos A Stamoulis

1. Coral reef management — Vanuatu.
2. Ecosystem management — Vanuatu.
3. Coral reefs and islands — Management — Vanuatu.
4. Marine resources conservation — Management — Vanuatu.
5. Marine ecology — Management — Vanuatu.

I. Delevaux, J.M.S. II. Stamoulis, K.A. III. Title IV. Pacific Community

577.220 99595 AACR2

ISBN: 978-982-00-1390-2

Citation: Delevaux, J.M.S. and Stamoulis, K.A. (2021) Assessment of ridge-to-reef management actions in Tagabe watershed and Mele Bay, Vanuatu. Suva, Fiji SPC, 52 pp

Produced by GEF Pacific International Waters Ridge to Reef Regional Project, Pacific Community (SPC), Suva, Fiji.

Layout and Design by Navneet Lal / Pacific Community (SPC)

Prepared for publication at SPC's Suva Regional Office, Private Mail Bag, Suva, Fiji, 2021

www.spc.int | spc@spc.int

Printed by Quality Print, Suva, Fiji, 2021

# CONTENTS

# ABBREVIATIONS

| | |
|---|---|
| BRT | Boosted Regression Trees |
| CCA | Community Conservation Area |
| DEM | Digital Elevation Model |
| GEBCO | General Bathymetric Chart of Oceans |
| GEM | Geoscience, Energy and Maritime |
| GIS | Geographic Information System |
| HYCOM | Hybrid Coordinate Ocean Model |
| IMM | Ifira Marine Management |
| InVEST | Integrated Valuation of Ecosystem Services and Tradeoffs |
| LULC | Land Use and Land Cover |
| MPA | Marine Protected Area |
| NAPA | National Adaptation Programme for Action |
| PDE | Percent Deviance Explained |
| CV PDE | Cross-validation Percent Deviance Explained |
| PCRAFI | Pacific Catastrophe Risk Assessment and Financing Initiative |
| R2R | Ridge to Reef |
| RapCA | Rapid Coastal Assessment |
| RUSLE | Revised Universal Soil Loss Equation |
| SDR | Sediment Delivery Ratio |
| SPC | Pacific Community |
| SST | Sea surface temperature |
| TPA | Terrestrial Protected Area |
| TSS | Total Suspended Sediment |

# LIST OF FIGURES

# LIST OF TABLES

# EXECUTIVE SUMMARY

Many Pacific Island nations support growing populations, which has led to increased pressure on marine and terrestrial resources. Urbanisation, commercial agriculture expansion and other land use activities are threatening coral reefs through increased sediment and nutrient runoff. Given limited resources for conservation and sustainable use of natural resources, accessible, easy-to-use conservation planning tools that are appropriate for island contexts are critically needed, especially those that incorporate land-sea linkages and consider human wellbeing.

We adapted and implemented a fine-scale (land: ~30 m x 30 m; sea: 30 m x 30 m) spatially-explicit decision-support framework in Mele Bay on Efate Island in Vanuatu, which covers the Tagabe watershed and the International Waters Ridge to Reef (IW R2R) project demonstration site in the country. The tool uses existing and newly collected datasets to identify where terrestrial conservation initiatives in the Tagabe watershed may have the greatest impact on marine conservation in Mele Bay. We tested proposed terrestrial restoration and marine protection scenarios and an urbanisation scenario in terms of their effects on coral reefs and fisheries. Although coral reefs can flourish in turbid waters, they are restricted to the top 4–10 m depth range and typically support fewer species, slower growth rates and poorer recruitment.

Our results supported previous studies in showing a negative effect of sediments on coral growth and abundance. We also found that sediments decreased fish biomass. Deforestation resulting from urbanisation and commercial agriculture expansion increases sedimentation while forest restoration mitigates sedimentation. Accordingly, our models projected increases in both corals and fishes that scaled with the area of forest restored. More trees resulted in more corals and fishes. Marine protection was also shown to support fishery outcomes in terms of increased numbers of targeted fishes. Conversely, an increase in urbanisation (and associated deforestation) caused declines in coral and associated inshore and reef fisheries. A combination of terrestrial forest restoration and marine protection from fishing resulted in the best outcomes for coral reefs and associated reef fisheries in Mele Bay on Efate Island, Vanuatu.

# 1. INTRODUCTION

Many island societies are highly dependent on terrestrial and marine ecosystems for their livelihoods, cultural identity and wellbeing (Kueffer and Kinney 2017). Today, many Pacific Island nations support growing populations, which has led to increased pressure on fisheries as well as on terrestrial resources (Walker and Bellingham 2011). Across much of the tropics, urbanisation, logging and commercial agriculture expansion in particular are threatening coral reefs through increased sediment and nutrient runoff (Dauvergne 1998; Mather et al. 1998). Excess nutrients and sediments have been shown to impact coral reefs by promoting benthic algae growth and smothering corals, respectively (Fabricius 2005b; Houk et al. 2014; Smith et al. 2016b). These land-based impacts affect islanders in a number of ways, such as reducing food resources upon which many islanders depend for wellbeing (Eriksson et al. 2017). In response to those threats, ridge-to-reef management has been widely advocated to foster social-ecological resilience (Delevaux et al. 2019). Implementing ridge-to-reef management requires tools to understand the potential outcomes of management actions on land at sea (Klein et al. 2012; Stamoulis and Delevaux 2015).

To address this need, a local-scale decision support tool was developed to model the effects of proposed land and sea management actions in areas selected as priorities for management. Building on a previously developed national-scale (100 m x 100 m), spatially-explicit decision-support framework for quantifying the effect of sediment stream runoff on coral reefs across Vanuatu, this project downscaled (~ 30 m x 30 m), adapted and applied the tool to inform local-scale conservation actions at the sub-watershed scale in the Tagabe watershed and Mele Bay on Efate Island, Vanuatu. We calibrated this linked land-sea decision support tool to test whether proposed terrestrial/land use and marine conservation/restoration actions benefit or impact downstream coral reefs and associated ecosystem goods and services (e.g., fisheries). To do so, we determined the impacts of current land use and proposed/future conservation and restoration efforts from ridge to reef on coral reef ecosystems. The framework links the Integrated Valuation of Ecosystem Services and Tradeoffs Sediment Delivery Ratio (InVEST SDR) to seascape models through a water quality model calibrated to existing empirical and remote sensing data available for the region. This approach leveraged existing datasets and recently collected marine ecological surveys in Mele Bay to characterise the effects of planned management actions.

To support the ongoing R2R efforts in Vanuatu and provide management insights for linked watershed and reef systems, we addressed the following three research questions.

i. How does sediment runoff influence coral reef benthic and fish indicators?

ii. Where do forest restoration or forest loss from agriculture expansion and urbanisation impact coral reefs due to differences in sediment runoff?

iii. How do marine ecosystems respond to proposed marine management actions alone and in combination with forest and agriculture land use restoration and urbanisation scenarios?

# 2. METHODS

## 2.1 DECISION SUPPORT TOOL OVERVIEW

To inform land use conservation and restoration activities in terms of coral reef impacts, the effects of proposed management efforts on coral reefs are determined by coupling various management scenarios with an adapted linked land-sea modelling framework (Delevaux et al. 2018b) (Fig 1). The framework links InVEST SDR version 3.2 (Hamel et al. 2015a) to coral reef ecosystem state models calibrated to existing empirical and remote sensing data. First, we designed a land-based management scenario that represents the projection of forest restoration set out in the Tagabe watershed management plan, and a scenario showing deforestation due to future urbanisation (Eckardt et al. 2008) (Fig 1a). We also included a fishing closure scenario derived from the Ifira marine management plan (Fig 1b).

Second, we calibrated and applied the land-sea framework, which connects sediments and coral reef models. Although nutrients are associated with sediment runoff and agriculture expansion (Fabricius 2005b), we did not explicitly model nutrient runoff here. The linked land-sea decision support tool consists of three key components: 1) InVEST SDR; 2) water quality model; 3) coral reef models. Sediment export (t. $yr^{-1}$) was modelled at 30 m x 30 m resolution for each watershed using the InVEST SDR, based on current land use, topography, soil types and rainfall data (Fig 1c-d). The modelled sediment export was diffused from pour points representing stream mouths into the coastal zone using a Geospatial Information System-based water quality model to generate the total suspended sediment (TSS) raster data (30 m x 30 m) (t. $yr^{-1}$) (Fig 1e). The bathymetry map was coupled with Geographic Information System (GIS)-based models to characterise the marine environment at 30 m x 30 m in terms of habitat structure (Fig 1f-g).

To identify coral reef areas susceptible to the effect of sediment runoff, we modelled coral reef indicators as a function of marine habitat and water quality (represented by TSS). We focused on proxies of ecological resilience, thus the coral reef models were applied to three benthic indicators (coral, macroalgae and turf algae), known to respond to land-based runoff, and three fish indicators which represent important subsistence and/or cultural resources (Green and Bellwood 2009; Jupiter and Egli 2011; Smith et al. 2016b). Lastly, we undertook a spatial analysis to assess the potential recovery and/or impact of future scenarios within the Tagabe ridge to reef system on coral reefs to foster coral reef recovery and benefits (Fig 1i).

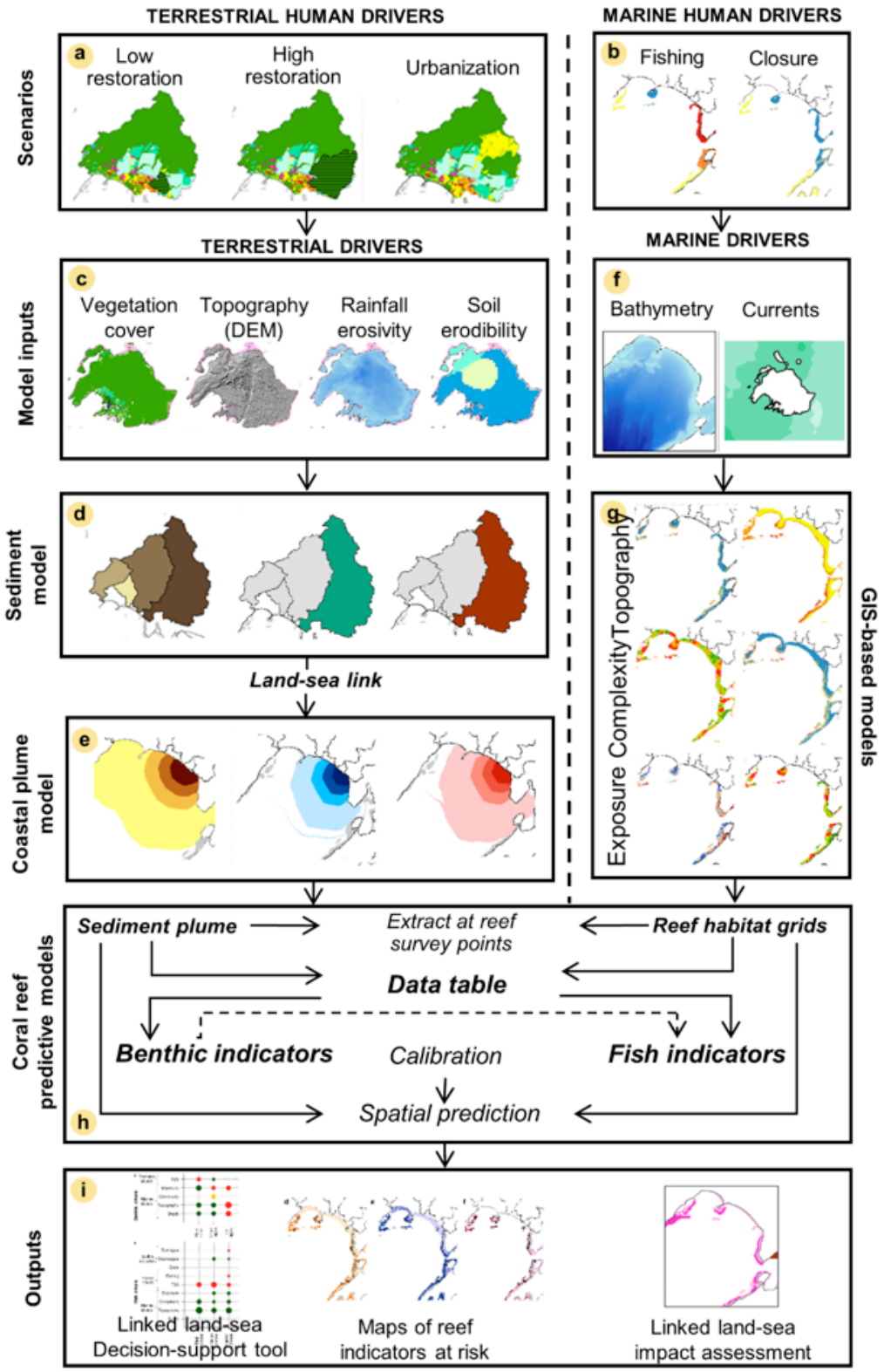


Fig 1. Ridge-to-reef modelling framework

(a) Land-use change scenarios were coupled with the linked land-sea decision support tool. (b) Marine management scenario. (c) Land cover, topography, rainfall and soil erodibility data were inputs in (d) the InVEST Sediment Delivery Ratio (SDR) model to quantify sediment export (t/yr). Sediment export values were assigned to (e) pour points at the shoreline and combined with (f) bathymetry and current maps into a coastal discharge model using GIS distance-based dispersion models to generate sediment plume maps (t/yr). Bathymetry and the habitat map were combined with (g) GIS-based models to derive the marine driver grid data (i.e. habitat topography, geography, exposure and complexity). (h) The coral reef predictive models were calibrated to coral reef survey data. (i) Outputs were: 1) a linked land-sea decision-support tool; 2) maps of benthic (% cover) and fish (g/m$^2$) indicators; and 3) a linked land-sea impact assessment.

## 2.2 SITE DESCRIPTION

The modelled land area represents four watersheds ranging in size from 628 ha to 6,231 ha with a total area of 12,276 ha (Fig 2). Topographically, the elevation of these watersheds ranges from 0 m to 254 m and averages 182 m (Fig S2a). Yearly rainfall varies between 182.4 mm/yr and 254.8 mm/yr and averages 205.9 mm/yr (Fig S2b). Based on a global database (Batjes 2016), there are three types of soils across the modelled area (Fig S2c).

Downstream in Mele Bay, the main currents flow from south to north and east to west (Fig S3a-b). The coral reef habitat area is spread across a total of 715 ha of mostly narrow reef systems which drop off quickly into deep water (Fig S3c-d). The Tagabe River catchment is the pilot site for Vanuatu's national R2R project (Fig 2c). It is a site of national significance as it is the only source of potable water for Port Vila's residents, including residential areas, businesses, agriculture and industry. The Tagabe watershed is under several environmental pressures, including deforestation due to urbanisation for new residential areas (Tawney 2006).

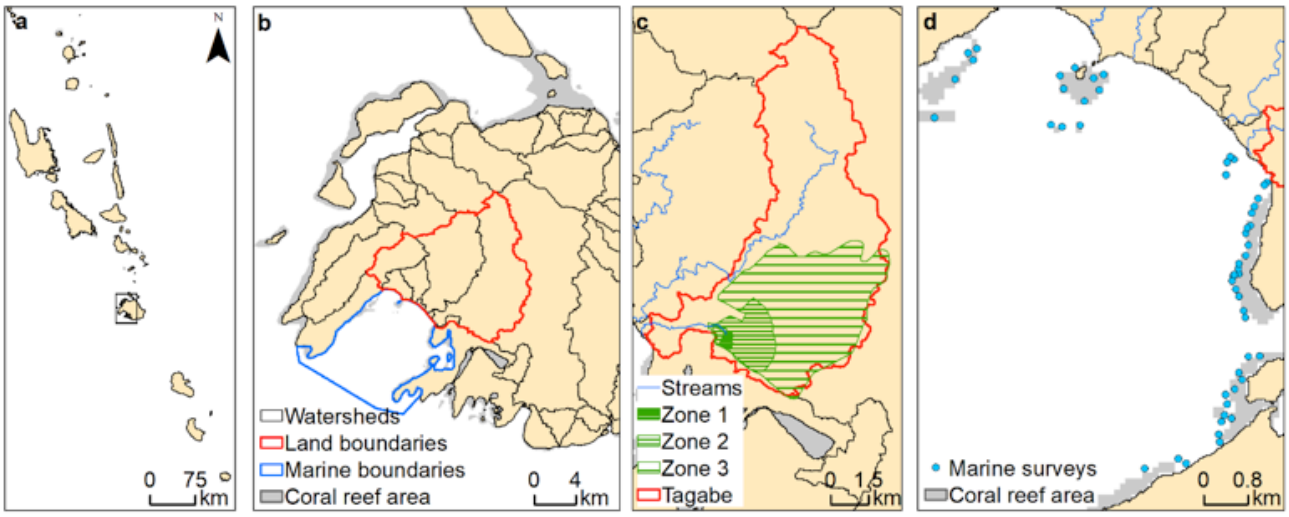


Fig 2. Study site

(a-b) Located on Efate island, the local-scale land-sea models were focused on Mele Bay and the watersheds that drain into it. (c) Restoration and urbanisation scenarios were implemented for the Tagabe watershed. (d) Marine surveys took place on the coral reefs of Mele Bay.

## 2.3 SCENARIO DESIGN

It is important to note that these scenarios are used to illustrate the potential effect of proposed management actions and reveal how land use change can affect soil erosion and downstream coral reefs. The scenarios are not meant to predict future land uses in any way, nor do they provide any recommendations for sustainable development.

### 2.3.1 Land-based scenarios

We considered two feasible land-use change scenarios (restoration and urbanisation) that represent alternative projected land use change in Tagabe watershed. The scenarios were designed based on the Tagabe watershed management plan, logging codes and urbanisation trends to inform ridge-to-reef management. The Tagabe River Catchment Management Plan (2017–2030) was officially launched in March 2018 to address pressing environmental issues and improve the management of the catchment to protect Port Vila's water supply. The management plan identified and established three Matnakara Water Protection Zones (MWPZ 1, MWPZ2 and MWPZ3) (WRD 2018). These zones

are designated for the protection of the quantity and quality of groundwater and land use practices are regulated in these areas. A recent Rapid Coastal Assessment (RapCA) found that the forest in Tagabe watershed is of high conservation value due to high endemism and the presence of critically endangered plant species, and thus it was recommended that it be declared a conservation area, thereby prohibiting all commercial activities (Sobey 2021). The Forestry Department has earmarked forest conservation and reforestation of the watershed as a high priority. Therefore, we considered a restoration scenario where we assumed conversion of current land uses to native forest in all three Water Protection Zones, as well as in a 30 m vegetation buffer along the Tagabe stream.

At the same time, deforestation is on the rise in Vanuatu and occurs primarily through human settlement and agriculture expansion (Eckardt et al. 2008). Approximately 80% of all deforestation takes place in low elevation terrain (<400 m) (Eckardt et al. 2008). The logging practices code of Vanuatu states that no deforestation should take place on slopes steeper than 30 degrees (McIntosh 2013). Over 90% of the detected deforestations are located within a perimeter of 3000 m around settlements, particularly in proximity to roads (Eckardt et al. 2008). Therefore, we considered an urbanisation scenario where deforestation takes place up to 3000 m around existing human land use and roads, and forest land use is converted to human land use (e.g., cultivated land, low density settlement and logging). The urbanisation scenario modelled human land use expansion (e.g., urban growth and agricultural expansion) in forested land cover on slopes primarily less than 30 degrees and below 400 m elevation in the Tagabe watershed. To comply with the existing logging practices code of Vanuatu, existing forest habitat along the Tagabe river was protected by a 30 m buffer and forest habitat within the declared conservation zones from the Tagabe management plan was retained.

### 2.3.2 Marine protection scenario

The National Adaptation Programme for Action (NAPA) seeks to promote community-based marine resource management to strengthen the adaptive capacities of coastal communities to climate and coastal changes. The development of the marine protection scenario was based on the Ifira Marine Protected Area (MPA) Management Plan provided by the Ifira Marine Management (IMM) team (IMMT 2019). The marine managed areas detailed in this document are currently in the registration process to become nationally recognised Community Conservation Areas (CCAs) with the Vanuatu Department of Environment. Therefore, these management actions represent the most likely future scenario of marine protection in the Mele Bay study area. The maps and information in the Ifira MPA Management Plan were used to develop a future scenario of fishing effort which was digitised in ArcGIS as a shapefile and then converted to a raster for use in spatial predictive models. While the plan did not specify specific management actions in each CCA, for modelling and planning purposes we assumed cessation of fishing in areas zoned as CCAs.

To map current fishing pressure, we conducted participatory mapping with local community members and project partners. Participants included Rodney Varsino Sope (Ifira Marine Management Field Head Supervisor), Nelson Bakokoto (Tanvasoko Environmental Officer), Ericksen Packett (R2R Project Manager) and Tom Maimai (Compliance Officer). Participants were shown a map of Mele Bay with delineated reef habitat areas and asked to rank the areas based on fishing pressure on a scale of zero to four, with zero representing MPAs and four representing the highest fishing pressure. We used this information along with field observations of fishing activity to create a shapefile representing current relative fishing pressure in Mele Bay that we converted to a raster and used as a predictor in the spatial predictive coral reef models.

## 2.4 SEDIMENT MODEL InVEST SDR

Erosion and overland sediment retention are natural processes that govern the sediment concentration in streams and nearshore regions. Sediment dynamics at the catchment scale are mainly determined by climate (rain intensity in particular), soil properties, topography and vegetation, and anthropogenic factors such as agricultural activities or dam construction and operation (Sharp et al. 2016). We leveraged the open-source InVEST toolbox from the Natural Capital Project for this study. SDR version 3.8 uses soil erosion equations to identify the land areas supplying sediment loads to stream mouths (Hamel et al. 2015b). We applied the InVEST SDR model to quantify the sediment export (t. $yr^{-1}$) to the coast by watershed due to soil loss on hillslopes from overland erosion (Hamel et al. 2015b) (Fig 1). SDR is spatially explicit and operates at the resolution of the Digital Elevation Model (DEM) input (30.7 m). For each pixel, the model first computes the amount of sediment eroded from that pixel using the Revised Universal Soil Loss equation (RUSLE), then computes the SDR to estimate the proportion of soil eroded on a given area that will travel to the stream mouth at the shoreline (see Appendix 3 for further details and Hamel et al. [2015] for full details on the model).

### 2.4.1 Land use mapping

We used satellite imagery available through ArcGIS online to create an updated land use map for the Mele Bay study area. A subset of land use classifications from the Pacific Catastrophe Risk Assessment and Financing Initiative (PCRAFI) land use map provided by the Secretariat of the Pacific Community (SPC) Geoscience, Energy and Maritime (GEM) division were used to apply supervised classification in ArcGIS by manually digitising land use polygons at a scale of 1:3000 (Table 1). The Cover Management Factor (C) represents the effect of vegetation on soil erosion rates (Renard et al. 1997). It is the ratio of soil loss of a specific crop to the corresponding soil loss under the condition of continuously fallow and tilled land (Renard et al. 1997).

Table 1. Land use/cover types and cover management (C) factors used in this study

| Land use/cover | C-factor | Source |
|---|---|---|
| Airport strip | 0.3 | 'Roads' (Rude et al. 2016) |
| Dirt road | 1 | 'Roads' (Rude et al. 2016) |
| Forest | 0.006 | 'Second growth forest with shrubs patches' (FAO 2007) |
| Golf course | 0.003 | (Falinski 2016) |
| Grassland | 0.014 | 'Pasto' c-factor, without grazing' (FAO 2007; Lianes et al. 2009) |
| Settlement (H) | 0.4 | (FAO 2007; Rude et al. 2016) |
| Settlement (L) | 0.1 | (FAO 2007; Rude et al. 2016) |
| Settlement (M) | 0.25 | (FAO 2007; Rude et al. 2016) |
| Open land | 1 | (Roose 1977; El-Swaify et al. 1982; Doheny et al. 2013) |
| Highway | 0.3 | 'Roads' (Rude et al. 2016) |
| Secondary roads | 0.4 | 'Roads' (Rude et al. 2016) |
| Shrubland | 0.013 | 'Potrero' (Lianes et al. 2009) |
| Tertiary roads | 0.6 | 'Roads' (Rude et al. 2016) |
| Tree plantation | 0.007 | (FAO 2007) |
| Agriculture | 0.3 | (Evensen et al. 2001; FAO 2007; Rude et al. 2016) |

## 2.5 WATER QUALITY MODEL

To model the impact of sediment runoff on coastal water quality, we generated a water quality map (30 m x 30 m) representing the total suspended sediment (TSS) from all watersheds discharging into Mele Bay for each land-use scenario. The sediment export from each watershed was diffused in coastal waters by adapting previously developed dispersal plume models in ArcGIS to represent the point source nature of stream discharge in the local coastal waters, accounting for depth and currents (Halpern et al. 2008; Delevaux et al. 2018a) (See Appendix 3 for further details).

## 2.6 CORAL REEF INDICATORS

To quantify coral reef resilience and fisheries, we considered the percentage cover of three benthic groups (scleractinian corals, turf algae and macroalgae) and the biomass of three fish groupings (g $m^{-2}$) based on their ecological roles and importance to local communities (IMMT 2019). The benthic indicators are known to respond to changes in land-based runoff, which in turn influence the distribution of fish taxa (Fabricius 2005b; Brown et al. 2017b), and therefore support aspects of coral reef ecological resilience and fisheries (Green and Bellwood 2009; Smith et al. 2016b). We considered total biomass of all fishes, biomass of targeted fish species and biomass of herbivorous fishes. We derived percentage cover of the benthic indicators and biomass of the fish indicators (g $m^{-2}$) from reef survey data collected by Seascape Solutions in November 2019 (see Table S2 for more details).

### 2.6.1 Field surveys

To effectively calibrate the seascape models with respect to sediment impacts, ecological surveys were conducted at 58 sample locations randomly placed on hard bottom habitats stratified by depth and distance from Tagabe stream using an equal random-stratified sample design (Hirzel and Guisan 2002) (Fig S1). Survey locations were randomly and equally allocated to three depth strata: shallow (1–5 m), moderate (5–12 m), and deep (12–21 m); and three distance strata: near (0–1.5 km), medium (1.5–3 km), and far (3–4.5 km). Pre-selected sample locations were uploaded to a GPS unit used to navigate to each start point in the field. Upon arrival at the survey location, two SCUBA divers entered the water and proceeded to the bottom. The first diver anchored the transect line at the start point and selected a compass heading for the transect which followed the depth contour. Headings were selected in a north-west direction unless the reef structure required laying the transect in the opposite direction. The diver then reeled out the transect line following the selected heading while identifying, counting and sizing all fishes observed within 2 m on either side of the transect line to a total of 50 m.

Fishes were identified to the lowest possible taxon and sizes were estimated to the nearest centimetre. The second diver maintained 10 m behind the first diver and took photos of the benthos every two metres along the transect for a total of 25 per transect. The photos were taken with a Canon S110 12-megapixel digital camera in underwater housing and oriented perpendicular to the substrate using a 0.8 m PVC monopod. When both divers completed their surveys, the fish diver proceeded to swim back along the transect counting mobile invertebrates within 2 m on either side of the line while the second diver followed, reeling in the transect line. Length estimates of fishes were converted to weight using the standard weight–length relationship and species-specific fitting parameters. Biomass estimates were summed at the transect level and converted to grams per square metre. Fishes were grouped by trophic group and based on whether they are targeted by fishers. Targeted status was determined by referring to fishery reports for the area (Amos 2007; Sobey 2021) as well as knowledge of targeted species in the South Pacific region (Table S2).

Benthic photos were processed using the Coral Point Count Extension (CPCe 4.1) software (Kohler and Gill 2006). Surface estimates expressed in per cent cover were derived from random stratified point count techniques using a nine points/$m^2$ ratio ensuring reliable habitat profiles with low bias and high precision (Dumas et al. 2009). Nine major habitat categories were considered, related to sediment type and live substratum coverage. These included live coral, coralline algae, macroalgae, turf, coral rubble, non-living substrate (sand, pavement, mud), echinoderms, and other (unknown) live substrate. Percentage cover was then aggregated at the transect level.

## 2.7 MARINE DRIVER MODELS

The marine driver grid maps (30 m x 30 m) were derived from bathymetry (SPC) maps for the site using GIS-based tools (Fig 2f-g). Based on existing literature, habitat characteristics (topography, complexity and exposure) were identified as important drivers of the modelled coral reef benthic and fish indicators (refer to Table S3 for more details on processing methods). Depth was derived from bathymetry at 5 m resolution (Roelfsema et al. 2013) using passive remote sensing techniques. Three types of habitat drivers, representing direct and indirect effects of seafloor topography on benthic and fish communities, were also derived from this bathymetry data (Roelfsema et al. 2013).

i. Habitat topography metrics, represented by slope computed for two neighbourhood sizes (30 m and 240 m radii), described the position of the reef relative to the surrounding area.

ii. Habitat complexity metrics that describe fine-scale topographic structure were represented by slope of slope, planar curvature and profile curvature. These were computed using the DEM Surface and Curvature Tools in ArcGIS (ESRI 2011b; Roelfsema et al. 2013).

iii. Habitat exposure metrics were used to characterise the direct and indirect effects of water flow due to seafloor topography and directionality.

These metrics were derived by computing seafloor aspect, the steepest downslope direction of the seafloor measured in degrees, using the Aspect tool in ArcGIS (ESRI 2011b; Roelfsema et al. 2013). We estimated exposure to winds by calculating the circular mean and standard deviation of aspect and converted the circular mean into measures of north and east using the sine and cosine functions, respectively, from the Spatial Analyst toolbox in ArcGIS (ESRI 2011b; Roelfsema et al. 2013).

## 2.8 SPATIAL PREDICTIVE CORAL REEF MODELS

We used Boosted Regression Trees (BRT) to generate the coral reef models (Franklin 2010) (Fig 2h). Tree-based models are effective at modelling nonlinearities, discontinuities (threshold effects), and interactions between variables, which is well suited for the analysis of complex ecological data (Breiman 1996, 2001; De'ath and Fabricius 2000). Since the coral reef indicators were all continuous variables, the response variables were modelled using a Gaussian (normal) distribution, and appropriate data transformations (square root for benthic indicators and fourth root for fish biomass) were applied to improve the normality of the distributions. Highly correlated ($r > 0.7$) environmental drivers were removed from the coral reef models (Stamoulis et al. 2018).

We calibrated the BRT models to locally collected coral reef data to determine the most influential drivers (among the simultaneously tested predictors) and estimated the underlying relationship between the modelled indicators and the key drivers using response curves (Elith et al. 2008; Venables and Ripley 2013). The values of the terrestrial and marine drivers' grid maps were sampled using bilinear interpolation at the location of each reef survey (centre of the transect) in ArcGIS. This approach takes a weighted average of the four nearest cell values, thereby accounting for the relative position of the reef surveys on the predictor grids and their different native spatial scales.

A BRT model was independently developed for each coral reef indicator using the values of the coral reef indicators and interpolated terrestrial and marine drivers at the reef survey locations. First, we calibrated the benthic indicator models as a function of the terrestrial and marine drivers. Then, we calibrated the fish indicators' models as a function of the terrestrial and marine drivers, as well as the empirical abundance of the three benthic groups. The calibration process used an internal ten-fold cross-validation to maximise the model fit and determine the optimal combinations of four parameters: 1) learning rate (lr); 2) tree complexity (tc); 3) bag fraction (bag); and 4) the maximum number of trees (see Elith et al. [2008] for more details).

We used the Percent Deviance Explained (PDE) and internal ten-fold cross-validation PDE (CV PDE) as performance measures of the model optimum. The optimal models explained the most variation in the response variables (i.e. greatest CV PDE) and were selected as the best and final models. The model calibration was conducted in R software using the gbm package (Ridgeway 2007; Elith et al. 2008; R Core Team 2014). Spatial autocorrelation of the response variables was tested using Moran's I Index for both the raw values and the ecological model residuals (Miller 2012).

Using the calibrated coral reef models, we predicted and mapped the distribution of each coral reef indicator on a cell-by-cell basis using the values of the terrestrial and marine drivers at each grid cell across the coral reef model domain. Predictive maps were generated for each indicator under present conditions and future scenarios (land-use change, marine management and combined scenarios) (Lovell et al. 2004; Hoeke et al. 2011). The coral reef predictive maps were generated at 30 m x 30 m. The boundaries of the coral reef model domains comprised the marine area of Mele Bay and the offshore boundary corresponded to the maximum surveyed depth (i.e. 21 m) (Fig 2b). First, we spatially predicted each benthic indicator as a function of its key drivers. Then, we spatially predicted the fish indicators as a function of their key drivers, including the predicted distribution of the benthic indicators.

To evaluate the quality of the coral reef model predictions, we compared the measured and predicted values of the coral reef indicators under present conditions. The values of the interpolated predictions and surveyed coral reef indicators at these locations were compared with a linear regression ($R^2$ and p-value). The predicted values of the benthic and fish grid maps were sampled using bilinear interpolation at the location of each reef survey (centre of the transect) in ArcGIS, thereby accounting for the relative position of the reef surveys on the predicted grids. Then, we overlaid the predicted maps with the survey point values for each indicator using the same colour ramp scale for the legend to enable visual comparison. The spatial predictions were performed in R software using the dismo and raster packages (Hijmans 2014; Hijmans et al. 2014; R Core Team 2014).

## 2.9 RIDGE-TO-REEF ASSESSMENT

We applied the framework as a decision-support tool using scenario planning to identify coral reef areas that could be affected by land use and/or marine management scenarios. To test how selected management actions (i.e. land or marine conservation areas and/or forest restoration areas) can foster coral reef resilience, the scenario impact assessment focused on three dimensions: 1) terrestrial impact (i.e. change in land use/land cover and sediment export); 2) water quality impact (i.e. change in TSS); and 3) marine impact (i.e. change in coral reef indicators).

i. First, we assessed and compared the difference between future scenarios and present (baseline) land uses, forest cover and human land uses.

ii. Second, we assessed and compared the difference between future scenarios and present (baseline) in terms of sediment export (t/yr).

iii. Third, we assessed and compared the change in TSS in terms of areas experiencing either an increase or decrease in TSS.

iv. Lastly, we calculated the differences between predictions of coral reef indicators under the land use change, marine management and combined scenarios, compared to present conditions.

We computed the significance of the pairwise differences per grid cell for each coral reef indicator relative to the mean and variance of all differences across the coral reef model domain using the SigDiff function from the R package SDMTools (Januchowski et al. 2010). The grid cells representing significant differences ($\alpha = 0.10$) were reclassified to indicate where predictions were significantly different from present conditions under each scenario. The areas of significant differences for each coral reef indicator were used to quantify the relative changes in benthic habitat and fish biomass within those areas.

Due to lack of data, nutrient runoff was not explicitly modelled in this study, but nutrients are known to bind and travel with sediment, thereby potentially contributing to lack of recovery from bleaching through the promotion of algae growth (i.e. synergistic effect) (Wooldridge 2009a; Wooldridge and Done 2009). However, given the limited understanding of these complex processes, we assumed that these effects were additive. Therefore, we applied the precautionary principle and considered these coral reef areas as vulnerable to cumulative impacts (Cooney 2004).

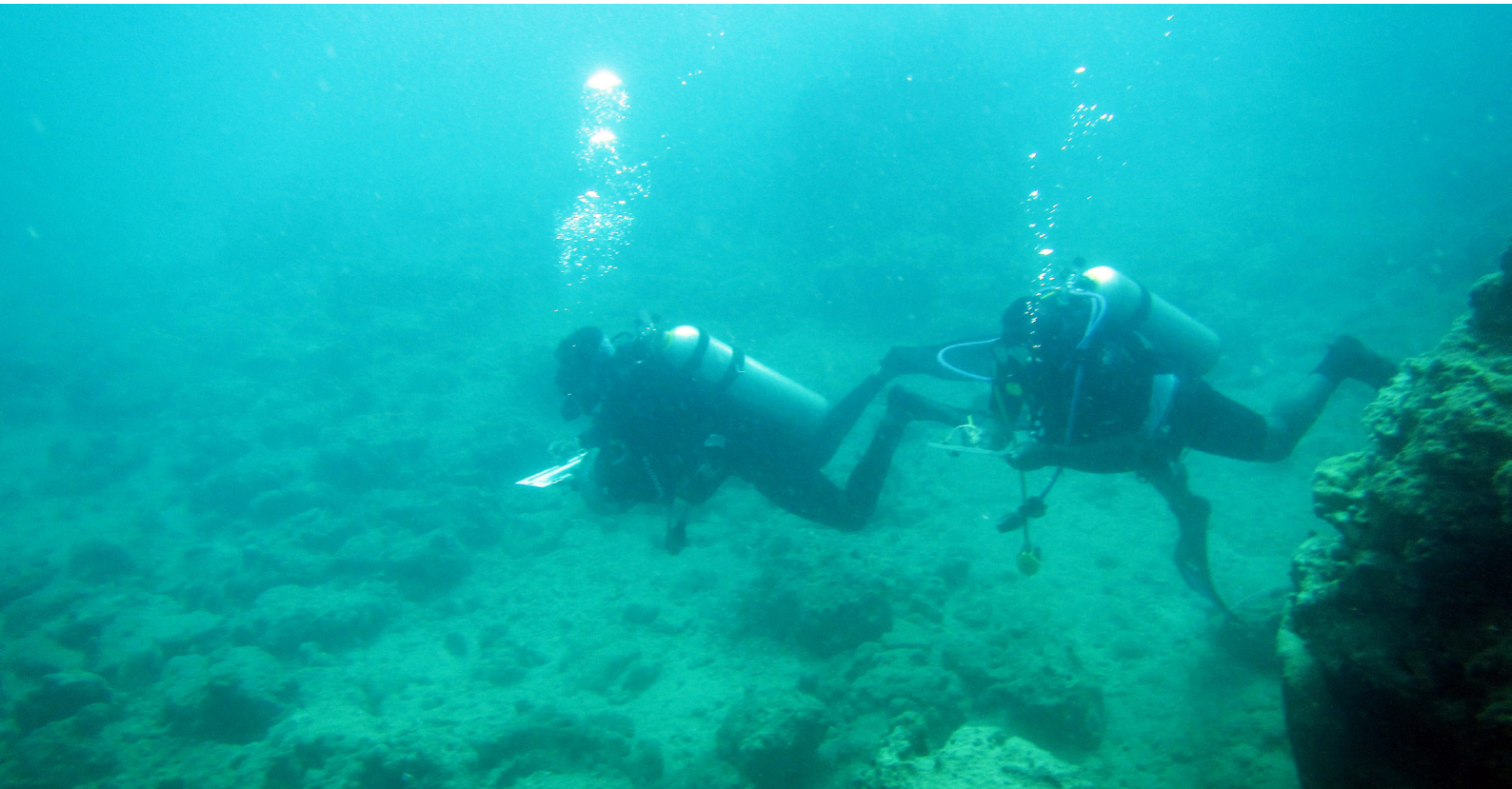

# 3. RESULTS

## 3.1 PRESENT RIDGE-TO-REEF CONDITIONS

Currently, the majority of land use/cover across the watersheds discharging into Mele Bay consists of forest (69.1%), grassland (14.8%), shrubland (7.3%), and human settlement and infrastructure (8.2%) (e.g. agriculture, golf course, roads and plantations) (Table S1 and Fig 3). The sediment export model under existing land use resulted in a total sediment export of 1258 t. $yr^{-1}$ (or 9.7 t/$km^{-2}$), with the Tagabe watershed discharging approximately 759 t. $yr^{-1}$ and therefore contributing 50% of the sediment load (Fig 3b). Consequently, the terrestrial human driver (represented by TSS) showed higher values of suspended sediment in the south-eastern side of Mele Bay (Fig 3c). The marine human driver (represented by fishing) depicts higher fishing pressure along the Tagabe reef and decreases towards the north and south west of Mele Bay (Fig 3d). In terms of the marine drivers, the depth of the marine habitats ranged from 0.1 m to 21 m, with habitats along the reef slopes of the barrier reefs being topographically more complex and habitats nearshore being flatter (Fig 3e-f and Fig S3). Reef habitats located to the north of the bay are more exposed to currents and wind (Fig 3g-h).

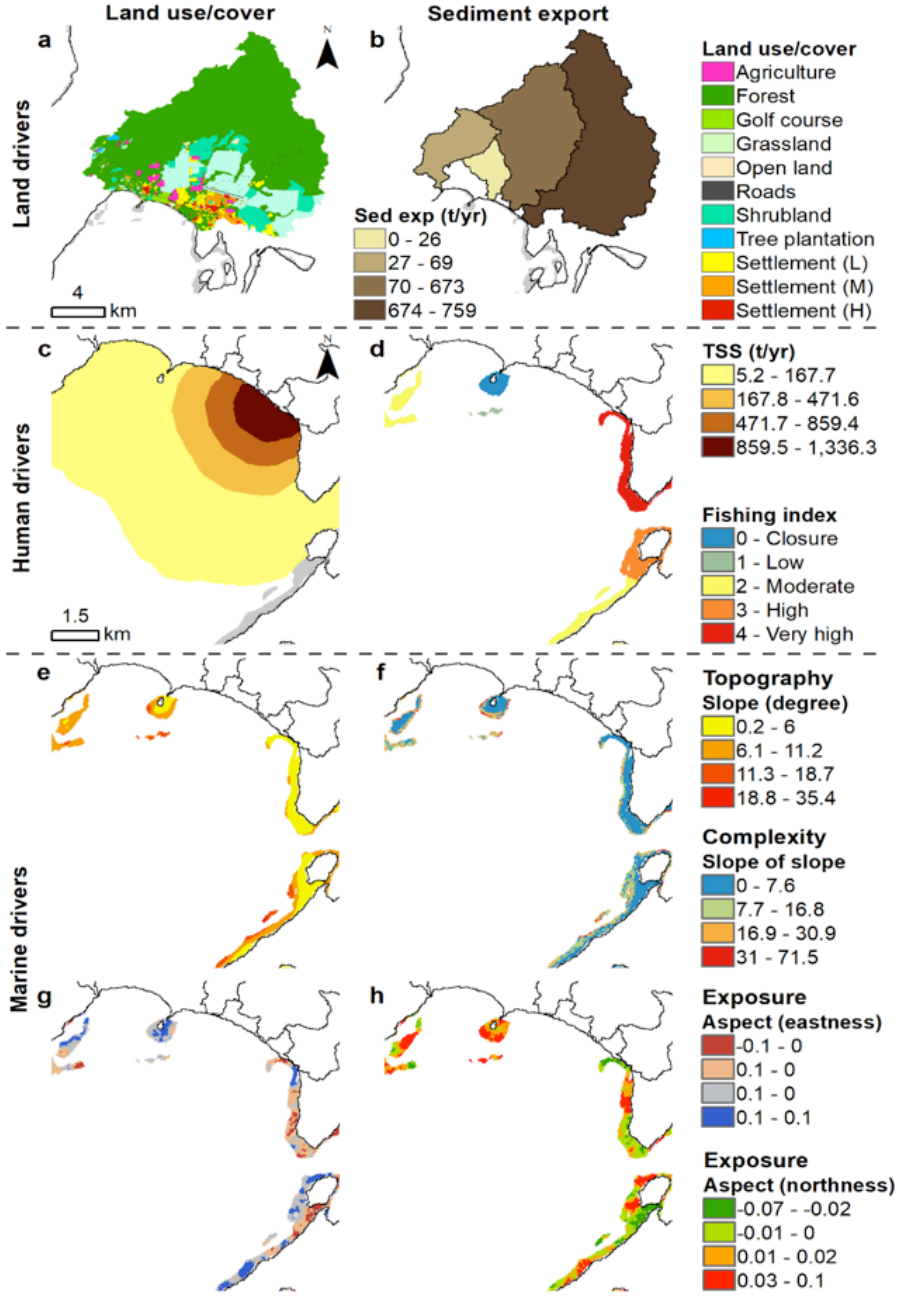


Fig 3. Present ridge-to-reef drivers

(a) Present land use/cover, (b) InVEST SDR results sediment export (t/yr) summarised by watershed. The human drivers are represented by (c) modelled TSS plumes (t. $yr^{-1}$) and (d) fishing pressure index. The marine drivers include (e) habitat topography (f) complexity, and exposure to wind and currents (g) eastness and (h) northness.

## 3.2 CORAL REEF PREDICTIVE MODELS

The PDE of the final coral reef models accounted for 44.6–92.6% and the internal CV PDE accounted for 17.0–47.7% (see Table S2 for more details). Analysis of the residuals from the final coral reef models showed no spatial autocorrelation (Moran's I Index $p > 0.1$). In terms of the terrestrial drivers, the coral reef models indicated that sediment runoff (represented by TSS) was a key driver of coral reef state (Fig. 4). TSS had a negative effect on coral and fish indicators and a positive effect on macroalgae cover. However, TSS was not selected as a key predictor for turf algae. In terms of the marine drivers, the coral reef models identified depth, habitat topography and complexity as key drivers of coral reef state (Fig. 4). The coral reef models also showed that macroalgae was positively associated with the herbivore and targeted fish groups (Fig. 4). Corals and macroalgae were positively associated with depth, while turf algae were negatively associated with depth. Most benthic and all fish indicators were positively associated with steeper, deeper reef slopes and more complex habitat, except for macroalgae, which showed a nonlinear relationship with habitat complexity.

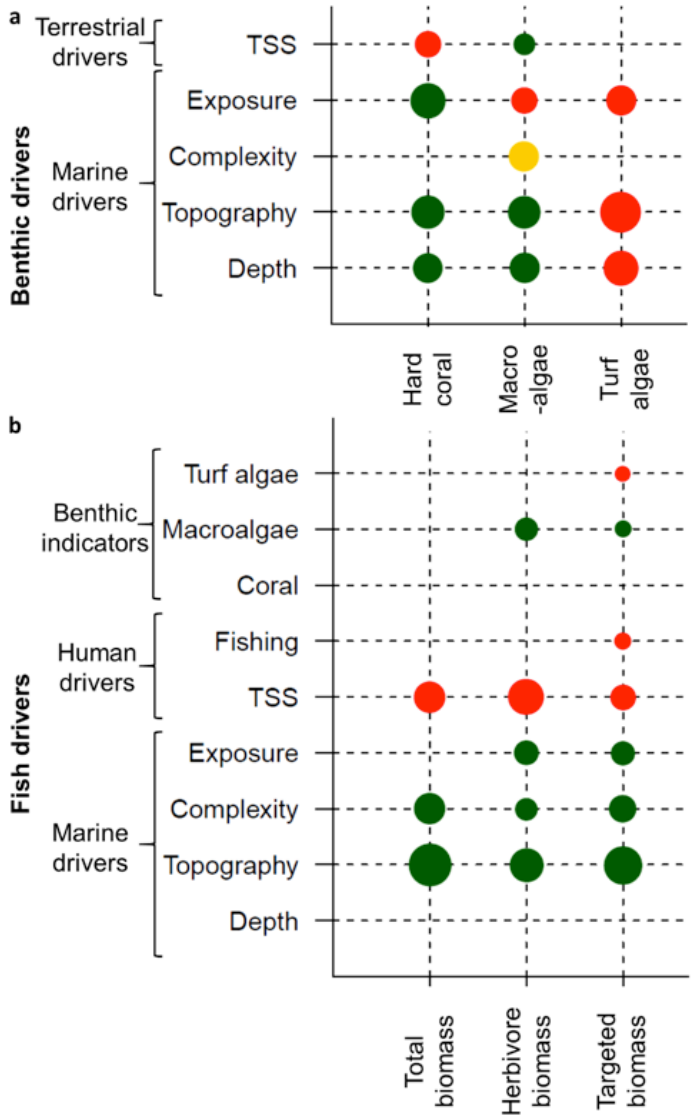


Fig 4. Coral reef predictive models

(a) Benthic and (b) fish predictive models for each site. The benthic and fish indicators are represented along the x-axes. The terrestrial and marine drivers (Fishing and TSS being driven by human actions), and benthic community (for the fish models) are represented on the y-axes. The marine drivers include metrics related to habitat exposure, complexity, topography and local geography (depth). The bubble size represents the relative percent contribution of each driver and the colour indicates whether the relationship between the indicator and the driver is positive (green), concave/convex (yellow), or negative (red).

## 3.3 SPATIAL PREDICTIVE MAPS OF CORAL REEF INDICATORS

The comparison of the predicted coral reef indicator values and empirical survey values showed moderately high $R^2$ values (ranging from 0.21–0.77), and statistically significant relationships for all indicators (see Fig. 5 for more details). The $R^2$ was higher for coral predictions compared to turf and macroalgae predictions, while the total and targeted fish biomass predictions performed better than the herbivore biomass. The BRT predictions well represented the empirically measured mean % cover (benthic) and biomass (fish) for all indicators across the entire study site (coral: 16.3%; macroalgae: 24.8%; turf algae: 50.1%; total biomass: 46.1 g/m$^2$; herbivore biomass: 23.0 g/m$^2$; targeted biomass: 28.4 g/m$^2$). Under present conditions, the coral reef models predicted a benthic community with lower coral cover (μ=12.3%; range = 1.8–44.9%), typically found along the reef slopes, compared to higher macroalgae cover (μ=22.1%; range = 2.9–68.5%), spatially more concentrated on the reef slopes and turf algae cover (μ=51.2%; range = 22.2–77.2%) higher on the reef flats and nearshore (Fig 5). The coral reef models predicted a fish community with a total biomass averaging 42.5 g/m$^2$ (range = 20.4–72.6 g/m$^2$), which accounted for herbivore biomass (μ=24.1 g/m$^2$, range = 4.8–43.0 g/m$^2$) and targeted fish biomass (μ=23.0 g/m$^2$, range = 3.4–68.5 g/m$^2$), found in higher numbers in more complex habitat away from Tagabe river (Fig 5).

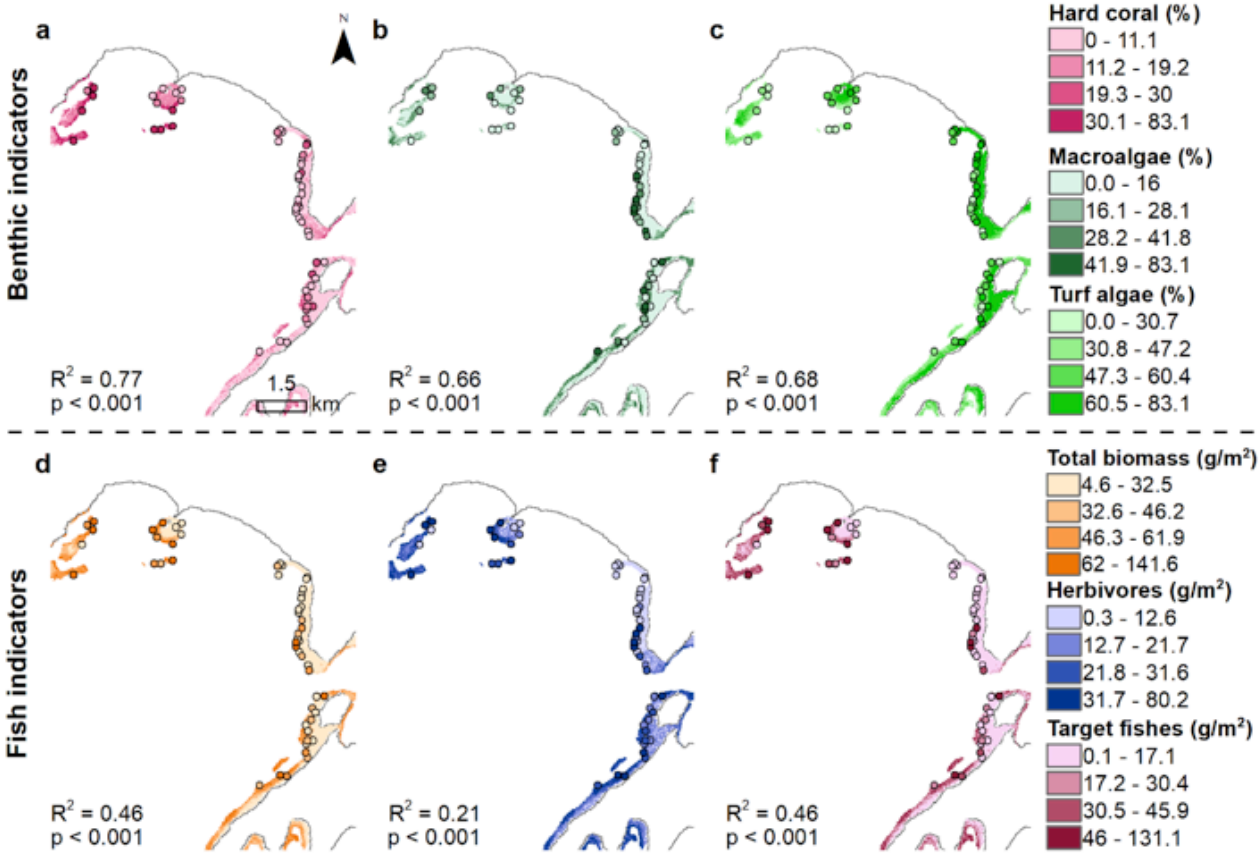


Fig 5. Observed and predicted distribution of coral reef indicators in Mele Bay under present conditions
Benthic indicators (a-c) are measured in % cover and the fish indicators (d-f) are measured in g m$^{-2}$. The predicted maps are overlaid with the survey points using the same colour ramp for visual comparison, combined with the $R^2$ and p-values.

## 3.4 TERRESTRIAL DRIVERS IMPACT ASSESSMENT

Under the restoration scenario, where 1330 ha of shrubland, grassland, open land and human settlement is restored to native forest in conservation zone 3 (Fig 6c), the sediment models indicated a decrease of 135 t. $yr^{-1}$ of sediment (18% decrease, Fig 6b), compared to current sediment export, resulting in a decrease in TSS around the Tagabe stream mouth (Fig 6c).

Under the urbanisation scenario, with low density human settlement expanded by 1342 ha, resulting in a key loss of 1330 ha of native forest (Fig 6d), the sediment models indicated an additional 5188 t. $yr^{-1}$ of sediment discharging at the shoreline (683% increase, Fig 6e), resulting in an increase of TSS in the southern and eastern sides of the bay (Fig 6f).

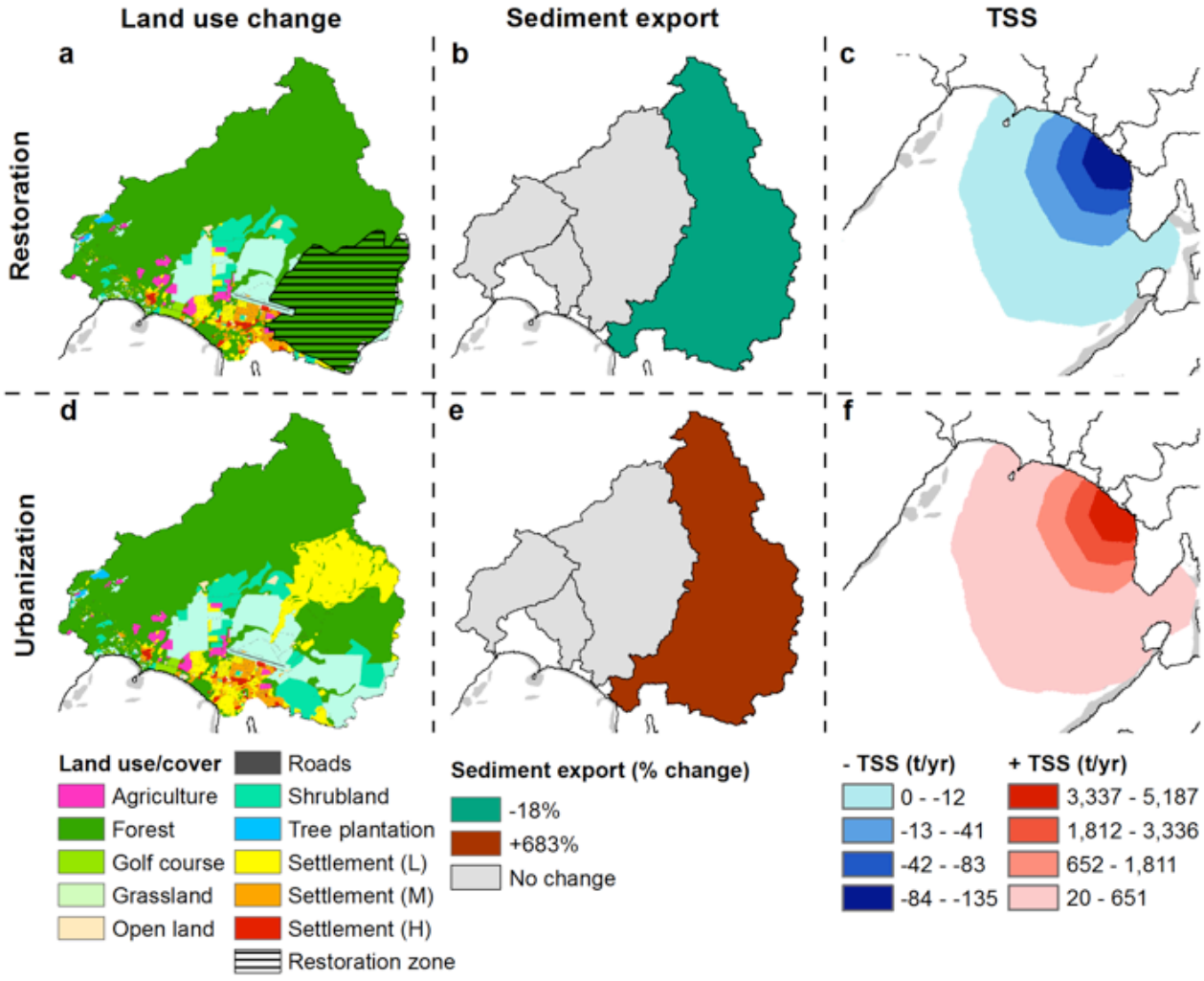


Fig 6. Mele Bay land use scenarios: change in land cover, sediment export and TSS
(a-c) restoration and (j-l) urbanisation.

## 3.5 CORAL REEF BENTHIC INDICATORS IMPACT ASSESSMENT UNDER LAND-USE CHANGE SCENARIOS

Under the restoration scenario, the coral reef models predicted a significant change of the benthic habitat over 18 ha (Table 2). This corresponds to an average increase of 7% for coral cover over 11 ha and an average decrease of 5% macroalgae cover over 12 ha (Table 2). The potential recovery of coral reef habitat is larger along the Tagabe reef and Ifira Island (eastern side of the bay), as well as Hideaway Island (northern side of the bay) (Fig 7).

Under the urbanisation scenario, the coral reef models predicted a significant change of the benthic habitat over 50 ha (Table 2). This corresponds to an average decrease of 20% for coral cover over 22 ha and an average increase of 17% for macroalgae cover over 29 ha (Table 2).

The potential impact on coral reef habitat is greatest on the southern part of Tagabe reef near the entrance to Vila bay and part of Ifira Island reef (eastern side of the bay), as well as Hideaway Island (northern side of the bay) (Fig 7). Turf algae did not change under any scenario because TSS was not selected as a key predictor. The habitat area (ha), average % cover change and standard deviation from the mean, predicted to significantly differ relative to present conditions, are reported for the benthic indicators per land-use change scenario.

Table 2. Coral benthic reef impact assessment

Habitat area (ha), average % change (in benthic cover), and standard deviation for areas predicted to significantly differ relative to present conditions are reported for each land use scenario. The total column shows the total area (ha) showing significant change accounting for spatial overlap amongst indicators. (Refer to Fig 7 for more details on relative change by benthic indicator spatially).

| Benthic indicators | Units | Hard coral | Macroalgae | Turf algae | Total |
|---|---|---|---|---|---|
| Restoration | ha | 11.3 | 11.7 | - | 17.6 |
| | % change | +7.0 | -5.1 | - | - |
| | std | ± 3.9 | ± 2.4 | - | - |
| Urbanisation | ha | 22.4 | 28.5 | - | 49.2 |
| | % change | -20.4 | +16.9 | - | - |
| | std | ± 9.3 | ± 7.0 | - | - |

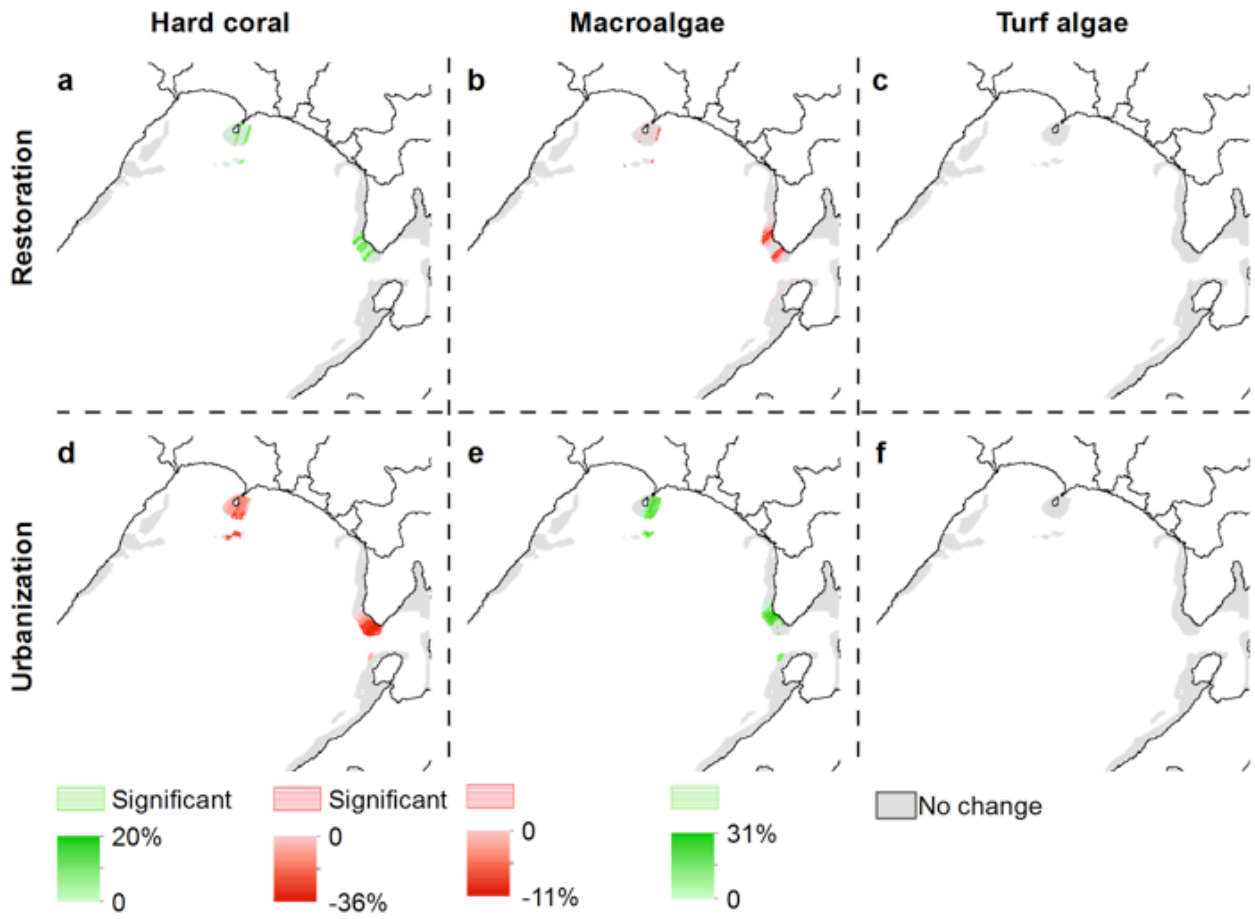


Fig 7. Maps of benthic indicators change per scenario: hard coral, macroalgae and turf algae

Relative change in benthic indicators abundance (% change) is shown under the (a-c) restoration and (d-f) urbanisation scenarios.

## 3.6 CORAL REEF FISH INDICATORS IMPACT ASSESSMENT UNDER LAND-USE CHANGE SCENARIOS

Under the restoration scenario, the coral reef models predicted a significant increase for fish biomass over a total of 31 ha (Table 3). This corresponds to increases of 4% for biomass of all fishes combined, 11% for herbivore biomass and 6% for targeted fish biomass (Table 3). The potential recovery of coral reef fishes is greatest along the Tagabe reef and Hideaway Island (northern side of the bay) (Fig 8).

Under the urbanisation scenario, the coral reef models predicted a significant loss of fish biomass over 76 ha (Table 3). This corresponds to losses of 22% for biomass of all fishes combined, 38% for herbivore biomass and 25% for targeted fish biomass (Table 3). The potential impact to coral reef fishes is larger along the Tagabe reef and Ifira Island (eastern side of the bay), as well as Hideaway Island (northern side of the bay) (Fig 8).

Table 3. Coral fish reef impact assessment under land-use change scenarios

Habitat area (ha), average % change (in biomass), and standard deviation for areas predicted to significantly differ relative to present conditions are reported for each land use scenario. The total column shows the total area (ha) showing significant change accounting for spatial overlap amongst indicators. (Refer to Fig 8 for more details on relative change by fish indicator spatially).

| Fish indicators | Units | All Fishes | Herbivores | Targeted | Total |
|---|---|---|---|---|---|
| Restoration | ha | 24.1 | 19.6 | 25.4 | 30.8 |
| | % change | +4.3 | +10.5 | +5.6 | - |
| | std | ±3.0 | ±6.4 | 3.4 | |
| Urbanisation | ha | 63.8 | 64.6 | 62.2 | 76.0 |
| | % change | -21.8 | -37.6 | -25.0 | - |
| | std | ±6.6 | ±11.0 | ±11.1 | |

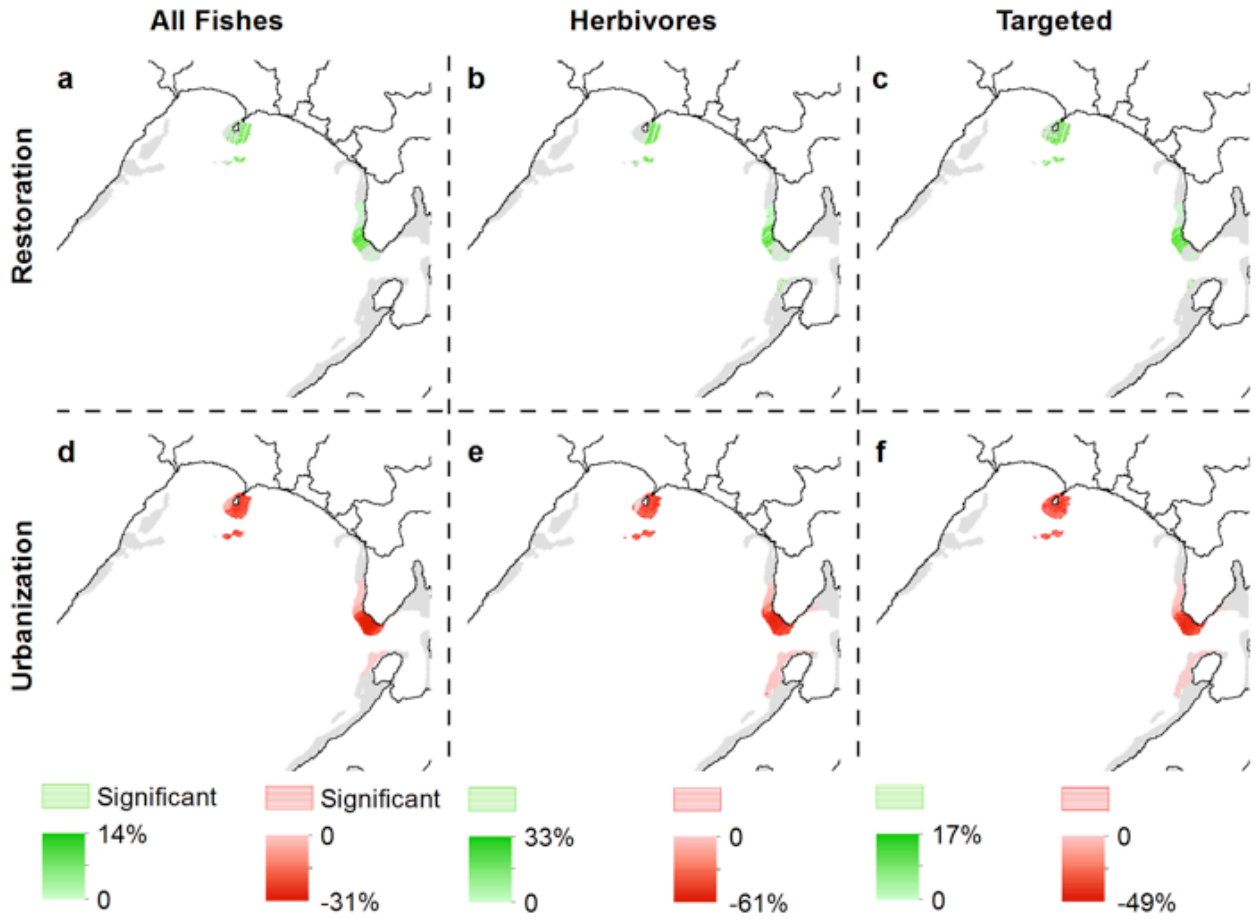


Fig 8. Maps of fish indicators change per land-use change scenarios: total biomass, herbivore biomass and targeted biomass

Relative change in fish indicator biomass (% change) is shown under the (a-c) restoration and (d-f) urbanisation scenarios.

## 3.7 CORAL REEF FISHERY IMPACT ASSESSMENT UNDER COMBINED MARINE AND LAND-USE CHANGE SCENARIOS

Under the marine management scenario (represented by closure), the coral reef models predicted a significant increase of 13% targeted fish biomass over 96 ha (Table 4). The potential recovery of targeted fishes is greatest along the Tagabe reef and around Ifira Island where the proposed management areas are to be located (Fig 9).

Under the combined marine management and restoration scenario, the coral reef models predicted a significant increase of 14% of targeted fish biomass over 90 ha (Table 4). The potential recovery of coral reef fishes is greatest along the Tagabe reef and Ifira Island (eastern side of the bay) where the proposed managed areas are to be located, as well as Hideaway Island (northern side of the bay), which is already managed as a no-take area (Fig 9).

Under the combined marine management and urbanisation scenario, the coral reef models predicted both a significant increase of 11% of targeted fish biomass over 40 ha and a significant decrease of 20% of targeted fish biomass over 63 ha (Table 4). The potential recovery of the reef fishery due to the marine closure is greatest along the northern portion of Tagabe reef (eastern side of the bay), in Fatumaru bay and around Ifira Island (Fig. 9). The potential impact to the reef fishery occurs on the southern portion of Tagabe reef and around Hideaway Island (northern side of the bay) (Fig 9). Despite the positive effect of the marine closure, the urbanisation scenario results in an overall decrease in targeted fish biomass.

Table 4. Coral reef fishery impact assessment

Habitat area (ha), average % change (in biomass), and standard deviation for areas predicted to significantly differ relative to present conditions are reported for each land use scenario. (Refer to Fig 9 for more details on relative change spatially).

| Combined scenarios | Units | Targeted Fish Increase | Targeted Fish Decrease |
|---|---|---|---|
| Closure + Present land use and land cover | ha | 95.9 | - |
| | % change | +13.1 | - |
| | std | ±2.8 | - |
| Closure + Restoration | ha | 90.4 | - |
| | % change | +14.1 | - |
| | std | ±5.0 | - |
| Closure + Urbanisation | ha | 39.8 | 62.5 |
| | % change | +10.8 | -20.2 |
| | std | ±2.5 | ±6.9 |

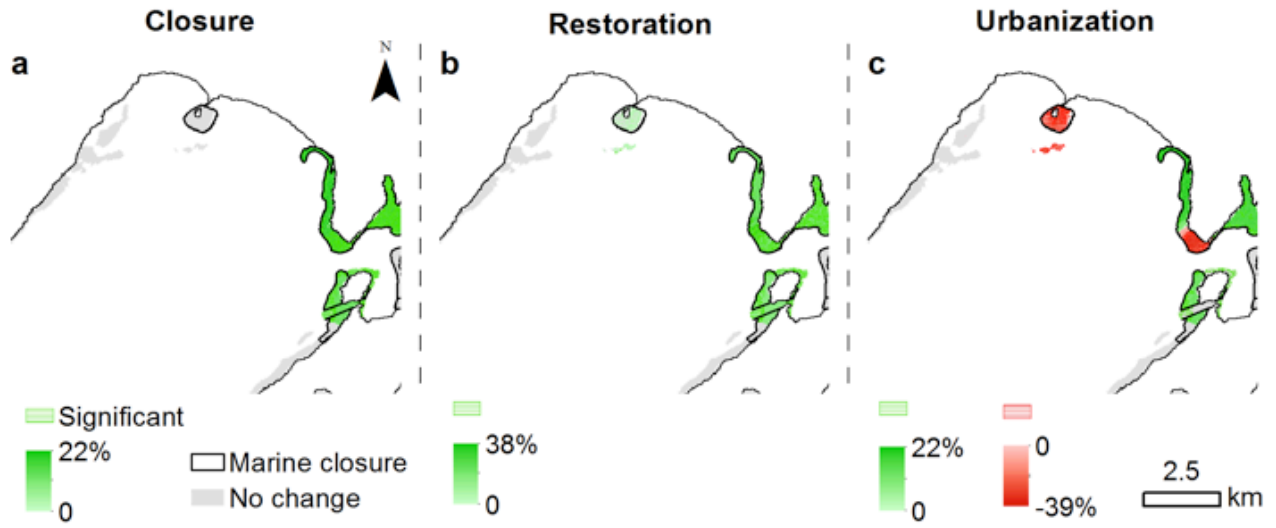


Fig 9. Maps of targeted fish indicator change under combined land use change and marine management scenarios

Relative change in targeted fish biomass indicator (% change) is shown under (a) marine management, (b) marine management combined with restoration, and (c) marine management combined with urbanisation scenario.

# 4. DISCUSSION

## 4.1 LAND-SEA MODELLING AND PLANNING

The linked land-sea decision-support tool identified reef areas vulnerable to land use/cover change and evaluated proposed management actions in terms of benefits to terrestrial and marine ecosystems. The modelling tool was first informed by data layers representing current conditions and these results represent the effect of current land use on sediment runoff once it enters the nearshore environment. Then, land use change and marine protection scenarios were applied to quantify the potential impact of TSS on reefs under increasing levels of forest restoration, increased urbanisation and marine closures.

The impacts of proposed terrestrial conservation and restoration actions vary between locations. However, land use actions can reduce soil erosion and provide benefits downstream, and can inform land-sea planning. This requires effective coordination across different agencies. Similarly, it is important to understand how marine conservation actions can help restore the fish communities which is important to local human wellbeing through food and cultural practices.

In Vanuatu, the Fisheries Department and the Department of Environmental Protection and Conservation have authority over coral reef ecosystems and the Department of Forests is mandated with the management of the forest sector, while local communities are also initiating marine conservation actions (IMMT 2019). This mismatch of governance and natural boundaries/processes can result in decision-makers having no control over activities outside their jurisdiction that impact the ecology of their systems (Jupiter et al. 2014). However, these results can facilitate discussions across agencies and inform stakeholders. The outputs are simple maps and spreadsheets, thereby allowing for more transparency in the decision-making process, which can foster community buy-in (Bremer et al. 2015).

## 4.2 LAND-SEA DECISION-SUPPORT TOOL

The land-sea tool calibration results established the effect of current land use, through sediment runoff, on coral reefs in the study area. The coral reef benthic models indicated that coral cover was negatively related to sediment exposure along with all the fish biomass indicators, while macroalgae cover, upon which herbivore and targeted fishes depend, was positively related to sediment exposure (Fig 4).

The adverse direct and indirect impacts of sedimentation and turbidity on benthic habitat at local scales has been well established (Fabricius 2005a). Increases in sediment can indirectly hinder competition for space by reef calcifiers (Smith et al. 2016a). Even if coral reefs in turbid waters can flourish (Anthony 1999), they are restricted to the top 4–10 m depth range (Yentsch et al. 2002; Fabricius et al. 2005), and typically support fewer species, slower growth rates and poorer recruitment (Rogers 1990). Coral reef fishes can be adversely affected by sedimentation and turbidity through altered foraging (Johansen and Jones 2013). Sedimentation and turbidity also indirectly affect coral reef fishes by altering the benthic community structure and composition (Rogers 1990).

The degree of dependence on different benthic groups may influence the susceptibility of fishes to habitat impacts from sediment runoff (Brown et al. 2017c), which can decrease or alter fish recruitment (DeMartini et al. 2013; Wenger et al. 2014). As a result, our coral reef predictions indicated that reefs closer to Tagabe stream, which discharges the highest amount of sediment in Mele Bay, generally support less coral abundance and fish biomass, in contrast to reefs located to the north west or south east sides of the bay, which support more coral abundance and fish biomass (Fig 5).

The reefs south of Tagabe stream experience higher fishing pressure as indicated by participatory mapping. One reason for this is that the chiefs of the Ifira clan, which holds traditional rights to the land there, have not made it available for development. As a result, there are no waterfront residents that prevent access and discourage fishing as along other parts of Mele Bay (Nelson Bakokoto pers. comm.) The relatively high fishing pressure is another factor which decreases fish biomass and has indirect effects on coral cover due to the removal of herbivores (Rasher and Hay 2010). Thus, the reefs in this area suffer from the cumulative impacts of both high sedimentation and high fishing pressure.

The calibration of the coral reef fish models established the effect of habitat and fishing pressure on coral reef fishes in the study area. The models indicated that targeted fish biomass was negatively related to fishing pressure (Fig 4). The adverse direct impact of fishing pressure on targeted reef fishes has been well established (Stamoulis et al. 2018). Fishing pressure alters the composition and trophic structure of marine ecosystems, and the resulting changes to functional groups can have strong effects on overall system resilience (Jackson et al. 2001; Green and Bellwood 2009). For example, removal of keystone herbivores can drive phase shifts to less desirable ecosystem states dominated by algae (Hoegh-Guldberg et al. 2007; Mumby 2009; Bahr et al. 2015).

Many studies have shown that habitat topography and complexity are primary drivers controlling coral reefs (Friedlander et al. 2003; Pittman et al. 2009; Stamoulis et al. 2018), as shown in Mele Bay where habitat topography and complexity were important predictors of fish biomass. Generally, fish biomass was higher along the reef slopes. Our results show that local-scale habitat characteristics played an important role in shaping these coral reefs.

## 4.3 LAND-SEA SCENARIO PLANNING

The scenario analysis results quantified the potential benefits of restoring native forest in the Tagabe watershed through reduced TSS risk to downstream coral reefs (Figs 7 and 8). Under the restoration scenarios, we showed that limiting human-derived sources of sediment in areas linked to coral reefs can improve coral reef habitat, while projected increases in urbanisation led to an increase in macroalgae and a loss of coral cover and fish biomass (Tables 2 and 3). Therefore, conserving and restoring forest in Tagabe conservation zones not only maintains good water quality essential for healthy coral reefs, it is also an important management strategy to mitigate the impacts of climate change on nearshore coral reefs within the range of sediment dispersal from rivers (McCook et al. 2001; Szmant 2002).

Our results indicated that marine conservation can reduce human impacts on coral reefs by increasing fish biomass within the marine closure (Halpern 2003; Delaney et al. 2017). Because targeted fishes are subject to fishing impacts, targeted fish biomass showed an increase under the marine closure scenario. Our results revealed that removal of fishing can enhance fish recovery under forest restoration scenarios or offset impacts of urbanisation on the targeted fish community. Although the impacts of urbanisation are reduced when coupled with the marine closure, our results indicated that land-based impacts can persist both inside and outside closure boundaries (Fig. 9).

These spatial trends imply that in the face of land-based impacts, marine closures alone are not always capable of addressing human drivers that impact the benthic community of coral reefs upon which reef fishes depend, reinforcing the need for ridge-to-reef management (Halpern et al. 2013).

## 4.4 AREA-BASED MANAGEMENT IMPLICATIONS

The spatially explicit models revealed that coral reefs in this area are sensitive to management actions at the local scale. This has important implications for future conservation planning and development in the Tagabe watershed and implies that accounting for finer spatial patterns is necessary to reduce impacts on coral reefs. The high resolution of our models allowed us to discover spatial nuances, which revealed the need for both marine and terrestrial management actions. Identifying where coral reefs are more or less vulnerable to local human impacts can inform place-based management actions to minimise risks (Game et al. 2008).

These results highlight that targeted terrestrial management in the Tagabe watershed can benefit terrestrial and marine ecosystems, particularly where marine closures may fall short, such as beyond the boundaries of the marine closure. This demonstrates the importance of accounting for the specifics of the place, such as geological history and rainfall (Selvarajah et al. 1994). In Mele Bay, conservation approaches should focus on protecting the reefs that are more vulnerable to sediment runoff and constitute important local fishing grounds for nearby coastal villages.

The results of this analysis correspond very well with the spatial management strategies outlined in the Ifira MPA Management Plan. The plan seeks to place protection from fishing on the reefs south of Tagabe river, which are subject to TSS impacts as well as high fishing pressure. Implementing upland management actions will decrease sediment export to these reefs and reducing or eliminating fishing pressure will support recovery. The plan also calls for ecosystem restoration activities such as coral transplantation and crown-of-thorns starfish removal which will further support coral reef ecosystem recovery in these areas. Furthermore, recent research found that coral reefs managed with high local community engagement and dependence on marine resources have a better chance of withstanding impacts related to climate change (Cinner et al. 2016).

We tested how sensitive our modelling framework was to the linkages between the SDR model and the plume models by running the framework with various c-factor values for the major land use types. We observed that the magnitude of change and the sizes of the spatial footprints of coral reef impacts as a function of sediment runoff varied depending on the c-factors used. However, the locations of coral reef impact from sediment runoff were consistently detected near the Tagabe watershed, which contributed the largest change in sediment export. Therefore, the potential benefits of forest restoration and/or marine conservation on downstream coral reef only changed in terms of amplitude.

In order to foster the resilience of these reefs, it is essential to consider minimising land-based impacts as research increasingly shows that marine closures are less effective when exposed to high land-based source pollution (Halpern et al. 2013; Wenger et al. 2015). Conservation planning should design protected areas that go beyond protecting parts of the ecosystem within their boundaries and instead augment resilience on a scale that transcends land-sea boundaries (Game et al. 2008). In this way, these findings reinforce that area-based ridge-to-reef management can reduce human impacts on coral reefs in the face of climate change.

# 5. CONCLUSION

Integrated land-sea planning requires the ability to trace where land-based pollutants come from and where they are likely to cause an impact once they enter the marine environment. This project adapted, applied and scaled down a linked land-sea decision-support tool (Delevaux et al. 2018a), to quantify, track and map the impact of land use change and marine conservation on coral reefs at the sub-watershed scale. The soils, rainfall and current data used in this study are from freely available global datasets, making this approach useful for regions with limited funding. In addition, this modelling framework relies on two freely available software packages (InVEST SDR and R) and the proprietary software ArcGIS (open access QGIS can be used as an alternative) (ESRI 2011a; Team 2014, 2015; Hamel et al. 2015b). By coupling this tool with scenario planning, we were able to test local conservation actions and forecast outcomes in terms of coral reef and fishery health.

We showed that limiting human-derived sources of sediment in areas linked to coral reefs can improve coral reef habitat, while increases in urbanisation will lead to an increase in macroalgae and a loss of coral cover and fish biomass. Therefore, conserving and restoring forest in Tagabe conservation zones supports healthy coral reefs and fisheries. Our results also revealed that removal of fishing can enhance fish recovery under forest restoration scenarios or offset impacts of urbanisation on the targeted fish community. Although the impacts of urbanisation are significantly reduced when coupled with the marine closure, our results indicate that land-based impacts can persist both inside and outside of closure boundaries. Therefore, a combination of terrestrial forest restoration and marine protection from fishing will result in the best outcomes for coral reefs and associated fisheries.

This information can be used to inform land-sea planning and help prioritise local conservation and management actions in the Tagabe watershed and Mele Bay. By simultaneously evaluating the effect of land use change, sediment runoff, fishing pressure, coral reef habitat and associated fish communities, this research highlighted the potential trade-offs and synergies arising between land and sea under different land-use scenarios. We applied land-use management scenarios based on proposed management actions in the study area to evaluate trade-offs and identify optimal management solutions. By adopting a ridge-to-reef conservation planning process, protected areas can be designed for multiple benefits that include improvements in biodiversity, drinking water and reef fisheries. The implementation of this approach in GIS allows managers to visualise and foresee the potential outcomes of management interventions. This type of approach has the potential to engender collaborative stewardship among agencies, communities and other stakeholders, and inform ecosystem-based, land-sea conservation planning in Vanuatu and other Pacific Island nations. The approach also provides a basis for ongoing research and modelling work to better identify and understand the impacts and trade-offs of other equally important models for potential interactions between land and sea continuum, which are currently poorly understood.

# 6. REFERENCES

Amos, M. 2007. Vanuatu fishery resource profiles. Apia, Samoa: Secretariat of the Pacific Regional Environment Programme.

Anthony, K. R. 1999. Coral suspension feeding on fine particulate matter. Journal of Experimental Marine Biology and Ecology 232:85–106.

Anthony, K. R. 2006a. Enhanced energy status of corals on coastal, high-turbidity reefs. Marine Ecology Progress Series 319:111–116.

Anthony, K. R., S. R. Connolly, and O. Hoegh-Guldberg. 2007. Bleaching, energetics, and coral mortality risk: Effects of temperature, light, and sediment regime. Limnology and oceanography 52:716–726.

Anthony, K. R. N. 2006b. Enhanced energy status of corals on coastal, high-turbidity reefs. Marine Ecology Progress Series 319:111–116.

Batjes, N. H. 2016. Harmonized soil property values for broad-scale modelling (WISE30sec) with estimates of global soil carbon stocks. Geoderma 269:61–68.

Borselli, L., P. Cassi, and D. Torri. 2008. Prolegomena to sediment and flow connectivity in the landscape: a GIS and field numerical assessment. Catena 75:268–277.

Braun, C. D., B. Galuardi, and S. R. Thorrold. 2018. HMMoce: An R package for improved geolocation of archival-tagged fishes using a hidden Markov method. Methods in Ecology and Evolution 9:1212–1220.

Breiman, L. 1996. Bagging predictors. Machine Learning 24:123–140.

Breiman, L. 2001. Statistical Modeling: The Two Cultures (with comments and a rejoinder by the author). Statistical Science 16:199–231.

Bremer, L. L., J. M. Delevaux, J. J. Leary, L. J. Cox, and K. L. Oleson. 2015. Opportunities and strategies to incorporate ecosystem services knowledge and decision support tools into planning and decision making in Hawai ʻi. Environmental management 55:884–899.

Brown, C. J., S. D. Jupiter, S. Albert, C. J. Klein, S. Mangubhai, J. M. Maina, P. Mumby, J. Olley, B. Stewart-Koster, and V. Tulloch. 2017a. Tracing the influence of land-use change on water quality and coral reefs using a Bayesian model. Scientific reports 7:4740.

Brown, C. J., S. D. Jupiter, H.-Y. Lin, S. Albert, C. Klein, J. M. Maina, V. J. Tulloch, A. S. Wenger, and P. J. Mumby. 2017b. Habitat change mediates the response of coral reef fish populations to terrestrial run-off. Marine Ecology Progress Series 576:55–68.

Brown, C. J., S. D. Jupiter, H.-Y. Lin, S. Albert, C. Klein, J. M. Maina, V. J. Tulloch, A. S. Wenger, and P. J. Mumby. 2017c. Habitat change mediates the response of coral reef fish populations to terrestrial run-off. Marine Ecology Progress Series 576:55–68.

Cavalli, M., S. Trevisani, F. Comiti, and L. Marchi. 2013. Geomorphometric assessment of spatial sediment connectivity in small Alpine catchments. Geomorphology 188:31–41.

Chicas, S., and K. Omine. 2015. Forest Cover Change and Soil Erosion in Toledo's Rio Grande Watershed. ISPRS-International Archives of the Photogrammetry, Remote Sensing and Spatial Information Sciences 40:353–358.

Dauvergne, P. 1998. Globalisation and deforestation in the Asia-Pacific. Environmental Politics 7:114–135.

De'ath, G., and K. E. Fabricius. 2000. Classification and Regression Trees: A Powerful yet Simple Technique for Ecological Data Analysis. Ecology 81:3178–3192.

Delevaux, J. M. S., S. D. Jupiter, K. A. Stamoulis, L. L. Bremer, A. S. Wenger, R. Dacks, P. Garrod, K. A. Falinski, and T. Ticktin. 2018a. Scenario planning with linked land-sea models inform where forest conservation actions will promote coral reef resilience. Scientific Reports 8:12465.

Delevaux, J. M. S., R. Whittier, K. A. Stamoulis, L. L. Bremer, S. Jupiter, A. M. Friedlander, M. Poti, G. Guannel, N. Kurashima, K. Winter, Robert, and K. Anders. 2018b. A linked land-sea modeling framework to inform ridge-to-reef management in high oceanic islands. Plos ONE.

Delevaux, J. M., K. A. Stamoulis, R. Whittier, S. D. Jupiter, L. L. Bremer, A. Friedlander, N. Kurashima, J. Giddens, K. B. Winter, and M. Blaich-Vaughan. 2019. Place-based management can reduce human impacts on coral reefs in a changing climate. Ecological Applications 29: e01891.

DeMartini, E., P. Jokiel, J. Beets, Y. Stender, C. Storlazzi, D. Minton, and E. Conklin. 2013. Terrigenous sediment impact on coral recruitment and growth affects the use of coral habitat by recruit parrotfishes (F. Scaridae). Journal of coastal conservation 17:417–429.

DeVantier, B. A., and A. D. Feldman. 1993. Review of GIS applications in hydrologic modeling. Journal of Water Resources Planning and Management 119:246–261.

Doheny, B., K. Maher, A. Minks, J. Rude, and M. Tyner. 2013. Ridge to Reef: Land Use, Sedimentation, and Marine Resource Vulnerability in Raja Ampat, Indonesia. Page 93. Conservation International and Bren School of Environmental Science and Management, UCSB.

Duarte, C. M., I. J. Losada, I. E. Hendriks, I. Mazarrasa, and N. Marbà. 2013. The role of coastal plant communities for climate change mitigation and adaptation. Nature Climate Change 3:961.

Dumas, P., A. Bertaud, C. Peignon, M. Leopold, and D. Pelletier. 2009. A "quick and clean" photographic method for the description of coral reef habitats. Journal of Experimental Marine Biology and Ecology 368:161–168.

Eckardt, R., M. Herold, J. Sambale, and S. Weaver. 2008. Monitoring deforestation patterns and processes in the Pacific island state of Vanuatu. Page 71 Geospatial crossroads GIF□orum'08: proceedings of the Geoinformatics Forum Salzburg. Wichmann.

Elith, J., J. R. Leathwick, and T. Hastie. 2008. A working guide to boosted regression trees. Journal of Animal Ecology 77:802–813.

Ellison, J. C. 1999. Impacts of Sediment Burial on Mangroves. Marine Pollution Bulletin 37:420–426.

El-Swaify, S. A., E. W. Dangler, and C. L. Armstrong. 1982. Soil erosion by water in the tropics.

ESRI. 2011a. ArcGIS Desktop: Release 10.4. Environmental Systems Research Institute, Redlands, CA.

ESRI. 2011b. ArcGIS Desktop: Release 10. Environmental Systems Research Institute. Redlands, CA.

Evensen, C. I., S. A. El-Swaify, C. W. Smith, and D. Flanagan, 2001. C-Factor development for sugarcane in Hawaii. Pages 687-690. American Society of Agricultural and Biological Engineers, Honolulu, HI, USA.

Fabricius, K., G. De'ath, L. McCook, E. Turak, and D. M. Williams. 2005. Changes in algal, coral and fish assemblages along water quality gradients on the inshore Great Barrier Reef. Marine Pollution Bulletin 51:384–398.

Fabricius, K. E. 2005a. Effects of terrestrial runoff on the ecology of corals and coral reefs: review and synthesis. Marine Pollution Bulletin 50:125–146.

Fabricius, K. E. 2005b. Effects of terrestrial runoff on the ecology of corals and coral reefs: review and synthesis. Marine Pollution Bulletin 50:125–146.

Falinski, K. A. 2016. Predicting sediment export into tropical coastal ecosystems to Support ridge to reef management. University of Hawaii at Manoa, Honolulu, Hawaii, USA.

FAO. 2007. Strategic environmental assessment. http://www.fao.org/docrep/007/y2413e/y2413e09.htm.

Fick, S. E., and R. J. Hijmans. 2017. WorldClim 2: new 1-km spatial resolution climate surfaces for global land areas. International journal of climatology 37:4302–4315.

Franklin, J. 2010. Mapping Species Distributions: Spatial Inference and Prediction. Cambridge University Press.

Friedlander, A. M., E. K. Brown, P. L. Jokiel, W. R. Smith, and K. S. Rodgers. 2003. Effects of habitat, wave exposure, and marine protected area status on coral reef fish assemblages in the Hawaiian archipelago. Coral Reefs 22:291–305.

Game, E. T., M. E. Watts, S. Wooldridge, and H. P. Possingham. 2008. Planning for persistence in marine reserves: a question of catastrophic importance. Ecological Applications 18:670–680.

Gholami, L., S. H. R. Sadeghi, and A. V. K. Darvishan. 2009. Modeling storm-wise sediment delivery ratio model in Chehelgazi watershed by using climatic and hydrologic characteristics. Journal of Agricultural Sciences and Natural Resources 16:253–260.

Green, A. L., and D. R. Bellwood. 2009. Monitoring functional groups of herbivorous reef fishes as indicators of coral reef resilience: a practical guide for coral reef managers in the Asia Pacific region. IUCN.

Halpern, B. S., K. A. Selkoe, C. White, S. Albert, and S. Aswani. 2013. Marine protected areas and resilience to sedimentation in the Solomon Islands. Coral Reefs 32:61–69.

Halpern, B. S., S. Walbridge, K. A. Selkoe, C. V. Kappel, F. Micheli, and C. D'Agrosa. 2008. A Global Map of Human Impact on Marine Ecosystems. Science 319:948–952.

Hamel, P., R. Chaplin-Kramer, S. Sim, and C. Mueller. 2015a. A new approach to modeling the sediment retention service (InVEST 3.0): case study of the Cape Fear catchment, North Carolina, USA. Science of the Total Environment 524:166–177.

Hamel, P., R. Chaplin-Kramer, S. Sim, and C. Mueller. 2015b. A new approach to modeling the sediment retention service (InVEST 3.0): Case study of the Cape Fear catchment. North Carolina, USA. Sci. Total Environ.

Hijmans, R. J. 2014. R package, Raster: Geographic data analysis and modeling. Software.

Hijmans, R. J. 2019. raster: Geographic Data Analysis and Modeling. R package version 2.9-23.

Hijmans, R. J., S. Phillips, J. Leathwick, and J. Elith. 2014. R package, dismo: Species distribution modeling.

Hirzel, A., and A. Guisan. 2002. Which is the optimal sampling strategy for habitat suitability modelling. Ecological modelling 157:331–341.

Hoeke, R. K., P. L. Jokiel, R. W. Buddemeier, and R. E. Brainard. 2011. Projected changes to growth and mortality of Hawaiian corals over the next 100 years. PloS one 6:e18038.

Houk, P., D. Benavente, J. Iguel, S. Johnson, and R. Okano. 2014. Coral Reef Disturbance and Recovery Dynamics Differ across Gradients of Localized Stressors in the Mariana Islands. PLOS ONE 9: e105731.

IMMT. 2019. Ifira Marine Protected Area Management Plan. Ifira Marine Management. Port Vila, Vanuatu.

Januchowski, S. R., R. L. Pressey, J. VanDerWal, and A. Edwards. 2010. Characterizing errors in digital elevation models and estimating the financial costs of accuracy. International Journal of Geographical Information Science 24:1327–1347.

Johansen, J. L., and G. P. Jones. 2013. Sediment-induced turbidity impairs foraging performance and prey choice of planktivorous coral reef fishes. Ecological Applications 23:1504–1517.

Jupiter, S. D., and D. P. Egli. 2011. Ecosystem-based management in Fiji: successes and challenges after five years of implementation. Journal of Marine Biology 2011.

Jupiter, S. D., A. P. Jenkins, W. J. L. Long, S. L. Maxwell, T. J. Carruthers, K. B. Hodge, H. Govan, J. Tamelander, and J. E. Watson. 2014. Principles for integrated island management in the tropical Pacific. Pacific Conservation Biology 20:193–205.

Klein, C. J., S. D. Jupiter, E. R. Selig, M. E. Watts, B. S. Halpern, M. Kamal, C. Roelfsema, and H. P. Possingham. 2012. Forest conservation delivers highly variable coral reef conservation outcomes. Ecological Applications 22:1246–1256.

Kohler, K. E., and S. M. Gill. 2006. Coral Point Count with Excel extensions (CPCe): A Visual Basic program for the determination of coral and substrate coverage using random point count methodology. Computers & Geosciences 32: 1259–1269.

Lianes, E., M. Marchamalo, and M. Roldán. 2009. Evaluación del factor C de la RUSLE para el manejo de coberturas vegetales en el control de la erosión en la cuenca del río Birrís, Costa Rica. Agronomía Costarricense 33:217–235.

López-Vicente, M., J. Poesen, A. Navas, and L. Gaspar. 2013. Predicting runoff and sediment connectivity and soil erosion by water for different land use scenarios in the Spanish Pre-Pyrenees. Catena 102:62–73.

Lovell, E., H. Sykes, M. Deiye, L. Wantiez, C. Garrigue, S. Virly, J. Samuelu, A. Solofa, T. Poulasi, K. Pakoa, and others. 2004. Status of Coral Reefs in the South West Pacific: Fiji, Nauru, New Caledonia, Samoa, Solomon Islands, Tuvalu, and Vanuatu. Status of coral reefs of the world 2:337–362.

Marois, D. E., and W. J. Mitsch. 2015. Coastal protection from tsunamis and cyclones provided by mangrove wetlands–a review. International Journal of Biodiversity Science, Ecosystem Services & Management 11:71–83.

Mather, A. S., C. L. Needle, and J. Fairbairn. 1998. The human drivers of global land cover change: the case of forests. Hydrological processes 12:1983–1994.

McIntosh, P. D. 2013. Review of soil and water provisions in the Papua New Guinea Logging Code of Practice and related codes in the tropics, A report under Project GCP. PNG/003/AUL for the PNG Forest Authority, the Food and Agriculture ….

Miller, J. A. 2012. Species distribution models: Spatial autocorrelation and non-stationarity. Progress in Physical Geography 36:681–692.

Morgan, K. M., C. T. Perry, J. A. Johnson, and S. G. Smithers. 2016. Nearshore Turbid-Zone Corals Exhibit High Bleaching Tolerance on the Great Barrier Reef Following the. Page 224.

Nagelkerken, I., G. Van der Velde, M. W. Gorissen, G. J. Meijer, T. Van't Hof, and C. Den Hartog. 2000. Importance of mangroves, seagrass beds and the shallow coral reef as a nursery for important coral reef fishes, using a visual census technique. Estuarine, coastal and shelf science 51:31–44.

Olley, J., J. Burton, V. Hermoso, K. Smolders, J. McMahon, B. Thomson, and A. Watkinson. 2015. Remnant riparian vegetation, sediment and nutrient loads, and river rehabilitation in subtropical Australia. Hydrological Processes 29:2290–2300.

Pierce, D. 2019. ncdf4: Interface to Unidata netCDF (Version 4 or Earlier).

Pittman, S. J., B. M. Costa, and T. A. Battista. 2009. Using Lidar Bathymetry and Boosted Regression Trees to Predict the Diversity and Abundance of Fish and Corals. J Coast Res:27–38.

R Core Team. 2014. R: A language and environment for statistical computing. R Foundation for Statistical Computing, Vienna, Austria.

Rasher, D. B., and M. E. Hay. 2010. Chemically rich seaweeds poison corals when not controlled by herbivores. Proceedings of the National Academy of Sciences 107:9683–9688.

Renard, K. G., G. R. Foster, G. A. Weesies, D. K. McCool, and D. C. Yoder. 1997. Predicting soil erosion by water: a guide to conservation planning with the Revised Universal Soil Loss Equation (RUSLE). United States Department of Agriculture Washington, DC.

Ridgeway, G. 2007. Generalized Boosted Models: A guide to the gbm package.

Roelfsema, C., S. Phinn, S. Jupiter, J. Comley, and S. Albert. 2013. Mapping coral reefs at reef to reef-system scales, 10s–1000s km2, using object-based image analysis. International Journal of Remote Sensing 34:6367–6388.

Rogers, C. S. 1990. Responses of coral reefs and reef organisms to sedimentation. Marine ecology progress series. Oldendorf 62:185–202.

Roose, E. J. 1977. Use of the universal soil loss equation to predict erosion in West Africa. Pages 60–74 Soil erosion: prediction and control. Soil Conservation Society of America Ankeny, IA.

Rude, J., A. Minks, B. Doheny, M. Tyner, K. Maher, C. Huffard, N. I. Hidayat, and H. Grantham. 2016. Ridge to reef modelling for use within land–sea planning under data-limited conditions. Aquatic Conservation: Marine and Freshwater Ecosystems 26:251–264.

Saunders, M. I., S. Atkinson, C. J. Klein, T. Weber, and H. P. Possingham. 2017. Increased sediment loads cause non-linear decreases in seagrass suitable habitat extent. PLOS ONE 12: e0187284.

Sharp, R., H. T. Tallis, T. Ricketts, A. D. Guerry, S. A. Wood, R. Chaplin-Kramer, E. Nelson, D. Ennaanay, S. Wolny, and N. Olwero. 2016. InVEST+ VERSION+ User's Guide. The Natural Capital Project. Stanford University, University of Minnesota, The Nature Conservancy, and ….

Sheppard, J. K., I. R. Lawler, and H. Marsh. 2007. Seagrass as pasture for seacows: Landscape-level dugong habitat evaluation. Estuarine, Coastal and Shelf Science 71:117–132.

Smith, J. E., R. Brainard, A. Carter, S. Grillo, C. Edwards, J. Harris, L. Lewis, D. Obura, F. Rohwer, E. Sala, and P. S. Vroom. 2016a. Re-evaluating the health of coral reef communities: baselines and evidence for human impacts across the central Pacific. Proc. R. Soc. B 283.

Smith, J. E., R. Brainard, A. Carter, S. Grillo, C. Edwards, J. Harris, L. Lewis, D. Obura, F. Rohwer, E. Sala, P. S. Vroom, and S. Sandin. 2016b. Re-evaluating the health of coral reef communities: baselines and evidence for human impacts across the central Pacific. Proc. R. Soc. B 283:20151985.

Sobey, M. 2021. Rapid Coastal Assessment of Tagabe River Catchment, Port Vila, Vanuatu. Page 34. Port Vila, Vanuatu.

Stamoulis, K. A., and J. M. S. Delevaux. 2015. Data requirements and tools to operationalize marine spatial planning in the United States. Ocean & Coastal Management 116:214–223.

Stamoulis, K. A., J. M. S. Delevaux, I. D. Williams, M. Poti, B. Costa, M. S. Kendall, S. J. Pittman, M. K. Donovan, L. M. Wedding, and A. M. Friedlander. accepted. Seascape models reveal places to focus coastal fisheries management. Ecological Applications.

Stamoulis, K. A., J. M. S. Delevaux, I. D. Williams, M. Poti, J. Lecky, B. Costa, M. S. Kendall, S. J. Pittman, M. K. Donovan, L. M. Wedding, and A. M. Friedlander. 2018. Seascape models reveal places to focus coastal fisheries management. Ecological Applications 28:910–925.

Tawney, E. J. 2006. Watershed Management and Planning in the Tagabe River Watershed Catchment Area in and around Port Vila, Vanuatu. MSc thesis., Michigan Technological University.

Team, Q. D. 2015. QGIS geographic information system. Open Source Geospatial Foundation Project, Versão 2.

Team, R. C. 2014. R: A language and environment for statistical computing. R Foundation for Statistical Computing.

Toonen, R. J., K. R. Andrews, I. B. Baums, C. E. Bird, G. T. Concepcion, T. S. Daly-Engel, J. A. Eble, A. Faucci, M. R. Gaither, M. Iacchei, J. B. Puritz, J. K. Schultz, D. J. Skillings, M. A. Timmers, and B. W. Bowen. 2011. Defining Boundaries for Ecosystem-Based Management: A Multispecies Case Study of Marine Connectivity across the Hawaiian Archipelago. Journal of Marine Biology 2011:13.

Tulloch, V. J., C. J. Brown, H. P. Possingham, S. D. Jupiter, J. M. Maina, and C. Klein. 2016. Improving conservation outcomes for coral reefs affected by future oil palm development in Papua New Guinea. Biological Conservation 203:43–54.

Venables, W. N., and B. D. Ripley. 2013. Modern Applied Statistics with S-PLUS. Springer Science & Business Media.

Walker, L. R., and P. Bellingham. 2011. Island Environments in a Changing World. Cambridge University Press.

Weatherall, P., K. M. Marks, M. Jakobsson, T. Schmitt, S. Tani, J. E. Arndt, M. Rovere, D. Chayes, V. Ferrini, and R. Wigley. 2015. A new digital bathymetric model of the world's oceans. Earth and Space Science 2:331–345.

Wenger, A. S., M. I. McCormick, G. G. Endo, I. M. McLeod, F. J. Kroon, and G. P. Jones. 2014. Suspended sediment prolongs larval development in a coral reef fish. Journal of Experimental Biology 217:1122–1128.

Wenger, A. S., D. H. Williamson, and T. E. Da. 2015. Effects of reduced water quality on coral reefs in and out of no-take marine reserves. Conservation Biology 30:142–153.

Williams, J. R. 1995. The EPIC model. Computer models of watershed hydrology: 909–1000.

Wilson, S. K., R. Fisher, M. S. Pratchett, N. A. J. Graham, N. K. Dulvy, R. A. Turner, A. Cakacaka, and N. V. C. Polunin. 2010. Habitat degradation and fishing effects on the size structure of coral reef fish communities. Ecological Applications 20:442–451.

Wischmeier, W. H., and D. D. Smith. 1978. Predicting rainfall erosion losses: a guide to conservation planning. Science and Education Administration, US Department of Agriculture.

Wooldridge, S. A. 2009a. Water quality and coral bleaching thresholds: Formalising the linkage for the inshore reefs of the Great Barrier Reef, Australia. Marine Pollution Bulletin 58:745–751.

Wooldridge, S. A. 2009b. Water quality and coral bleaching thresholds: Formalising the linkage for the inshore reefs of the Great Barrier Reef, Australia. Marine Pollution Bulletin 58:745–751.

Wooldridge, S. A., and Done. 2009. Improved water quality can ameliorate effects of climate change on corals. Ecological Applications 19:1492–1499.

WRD. 2018. Tagabe River Catchment Management Plan 2017-2030. Page 50. Port Vila, Vanuatu.

Yentsch, C. S., C. M. Yentsch, J. J. Cullen, B. Lapointe, D. A. Phinney, and S. W. Yentsch. 2002. Sunlight and water transparency: cornerstones in coral research. Journal of Experimental Marine Biology and Ecology 268:171–183.

Yu, C., J. A. Y. Lee, and M. J. Munro-Stasiuk. 2003. Extensions to least-cost path algorithms for roadway planning. Int J Geogr Inf 17:361–376.

# APPENDIX 1 - FIGURES

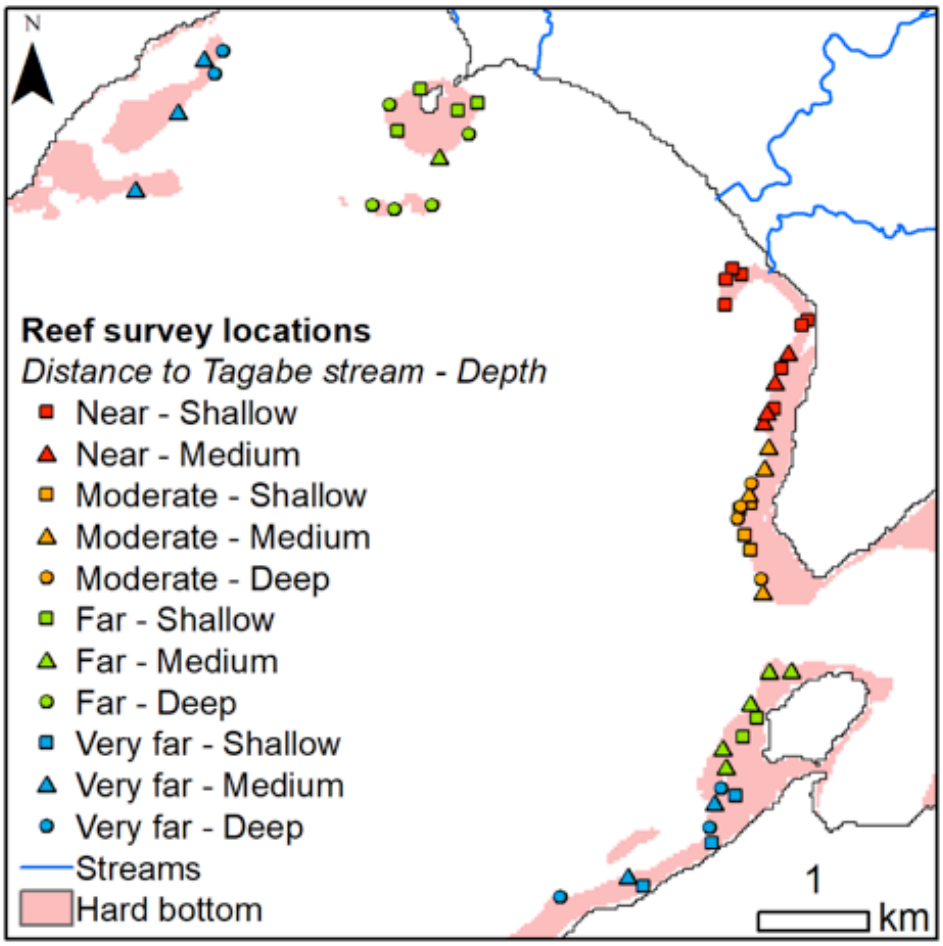


Fig S1. Coral reef survey locations identified by distance from Tagabe stream and depth strata.

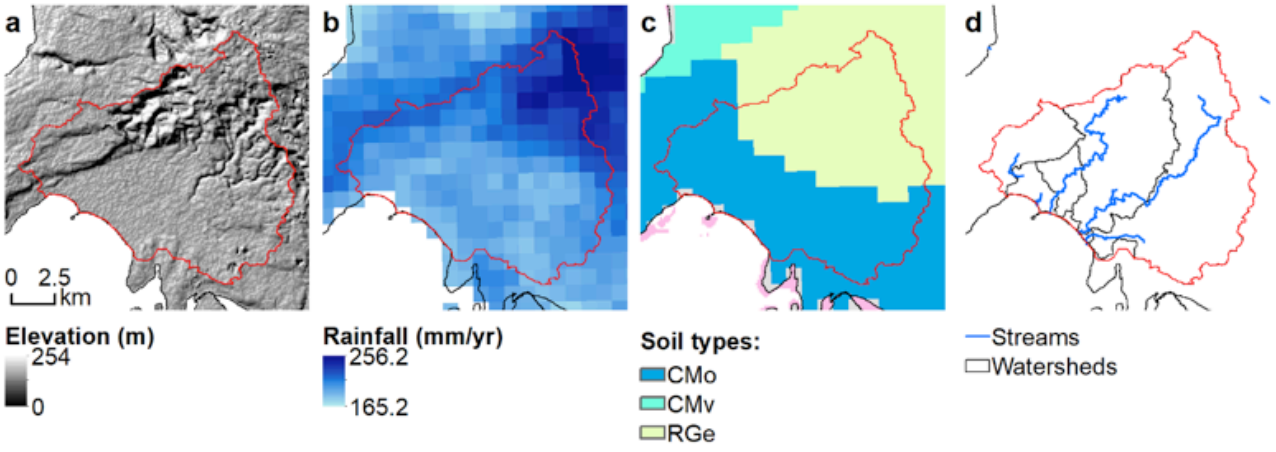


**Fig S2. Terrestrial geography & InVEST SDR inputs.** (a) Digital Elevation Model (DEM), (b) average yearly rainfall (mm/yr), (c) soil types, (d) streams and watershed boundaries within the area of interest.

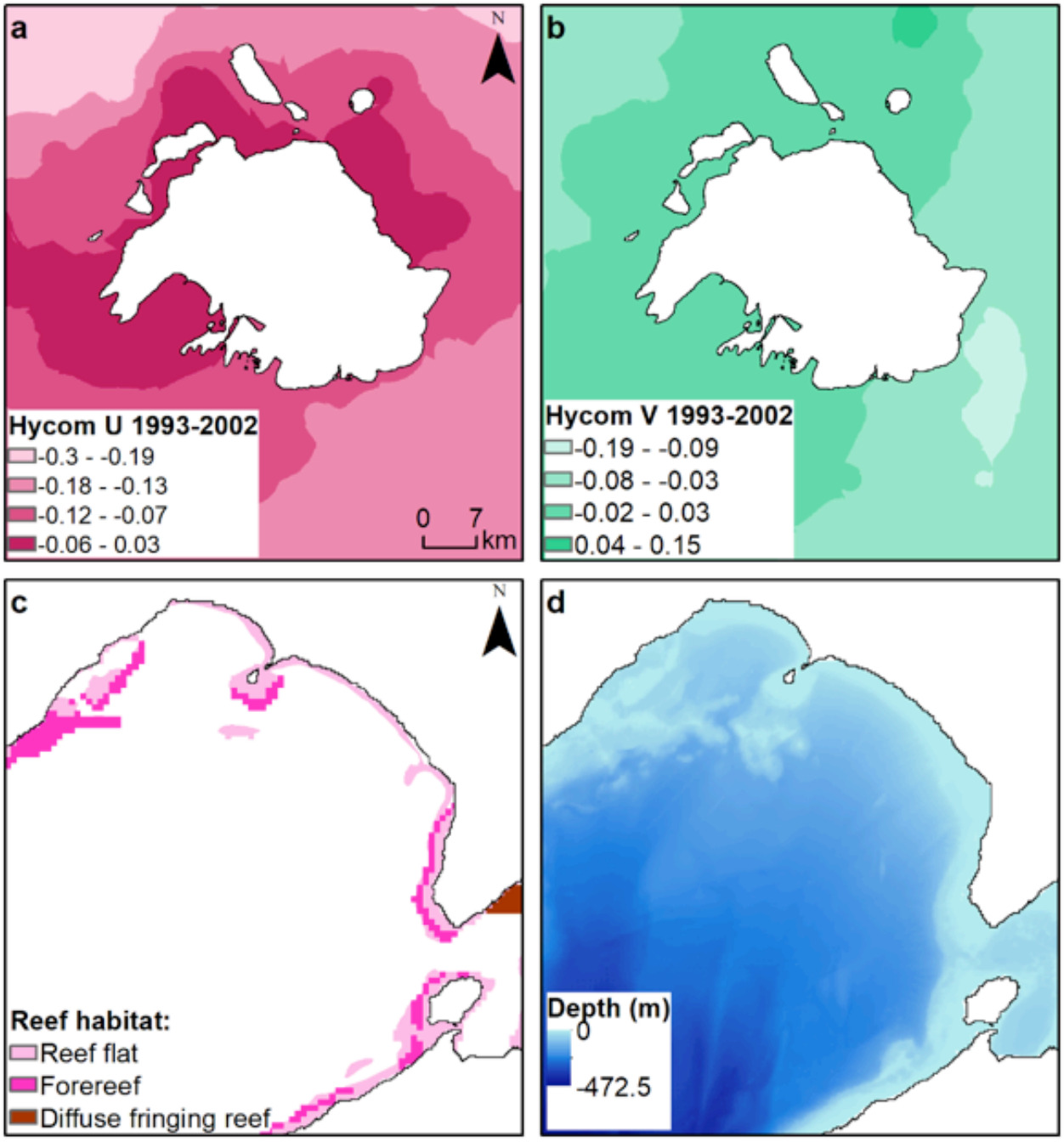


Fig S3. Marine geography variables. (a) East-west component of HYCOM surface currents, (b) north-south component of HYCOM surface currents, (c) bathymetry, (d) reef habitat.

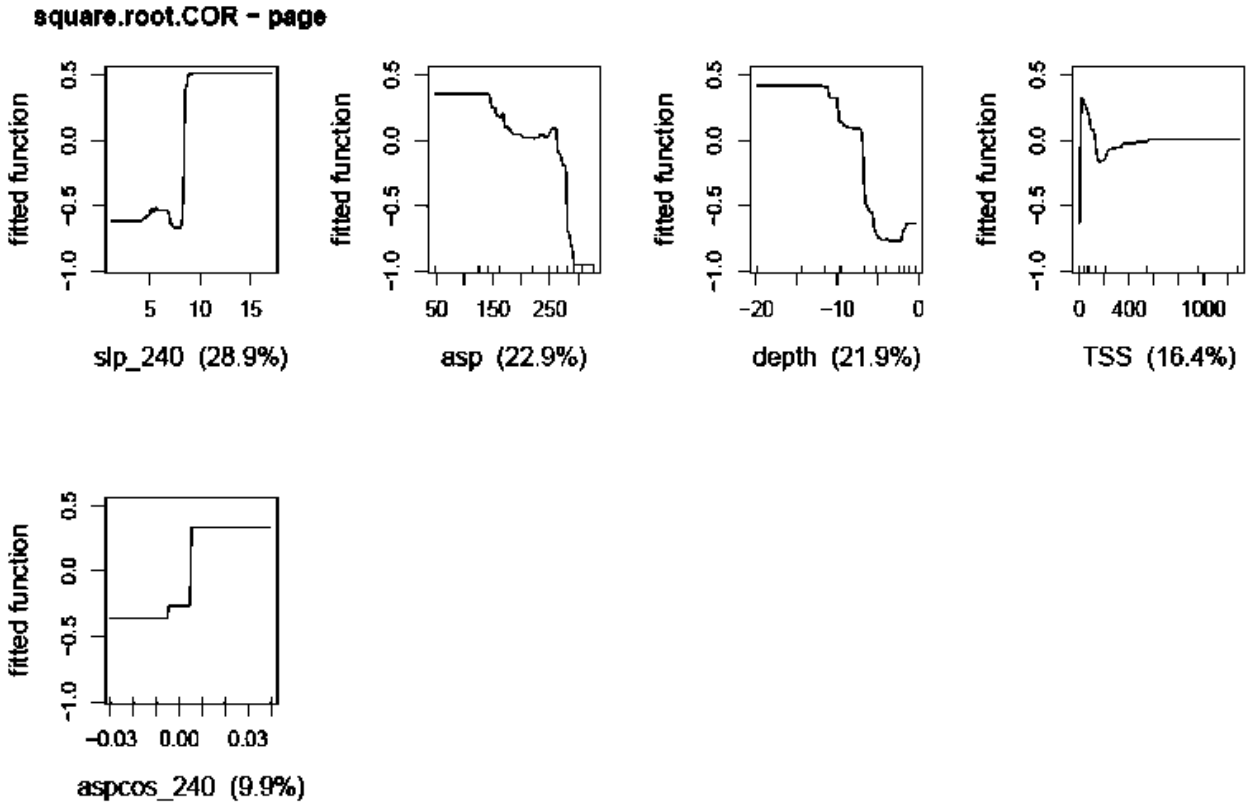


Fig S4. Response curves for coral. Curves show the relative relationships with selected terrestrial and marine drivers.

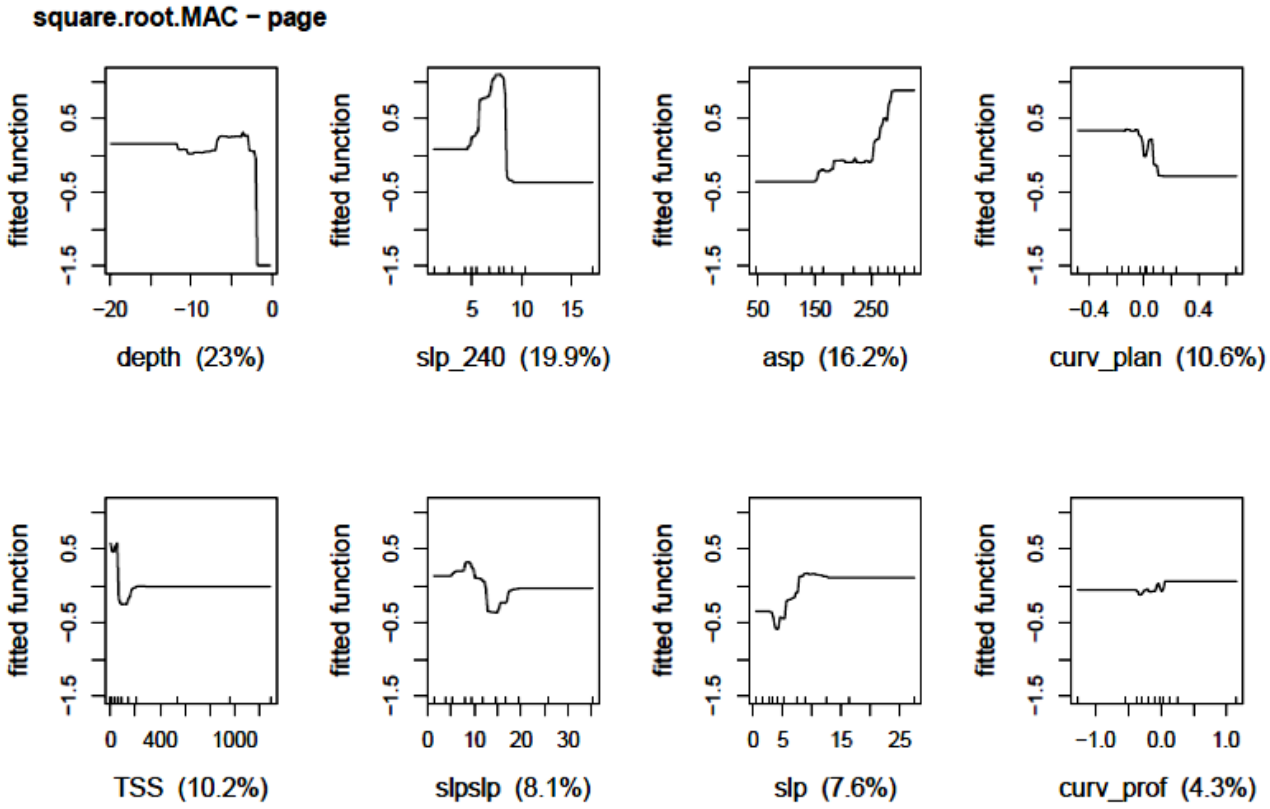


Fig S5. Response curves for macroalgae. Curves show the relative relationships with selected terrestrial and marine drivers.

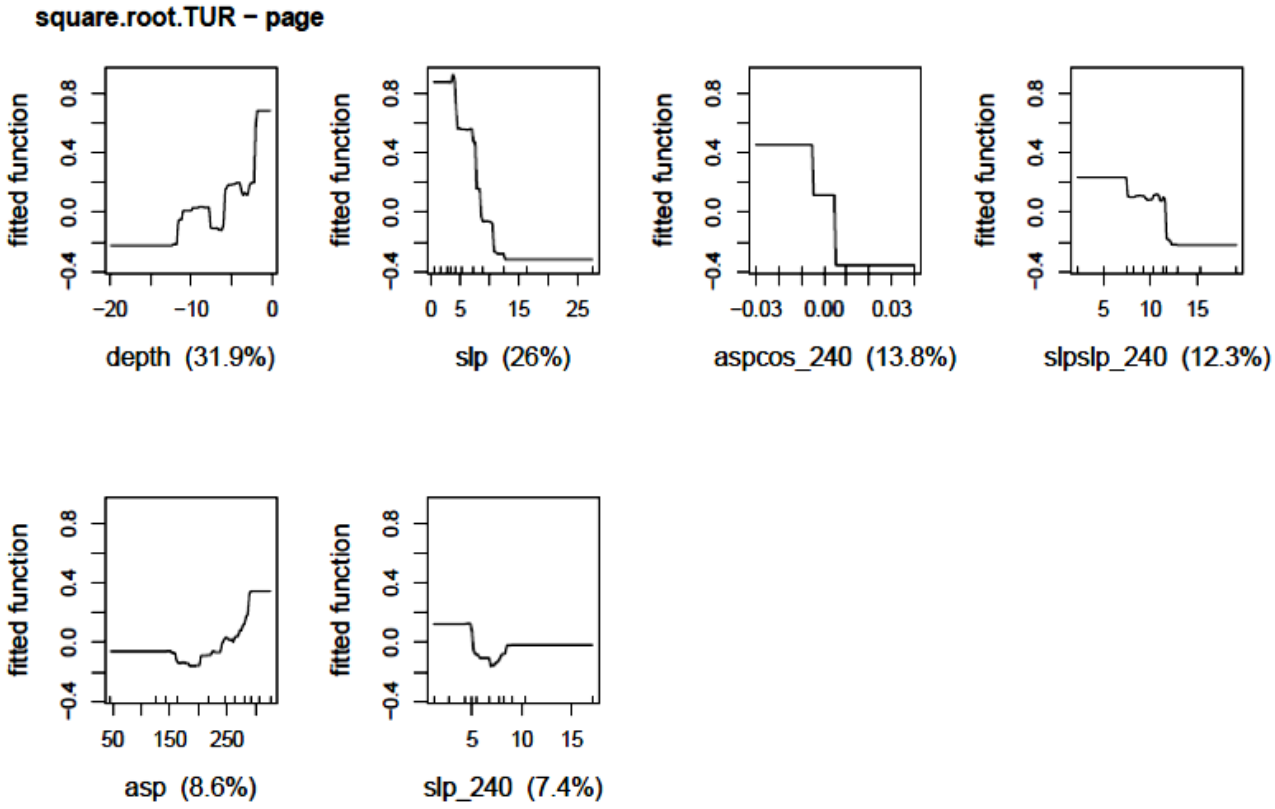


Fig S6. Response curves for turf algae. Curves show the relative relationships with selected terrestrial and marine drivers.

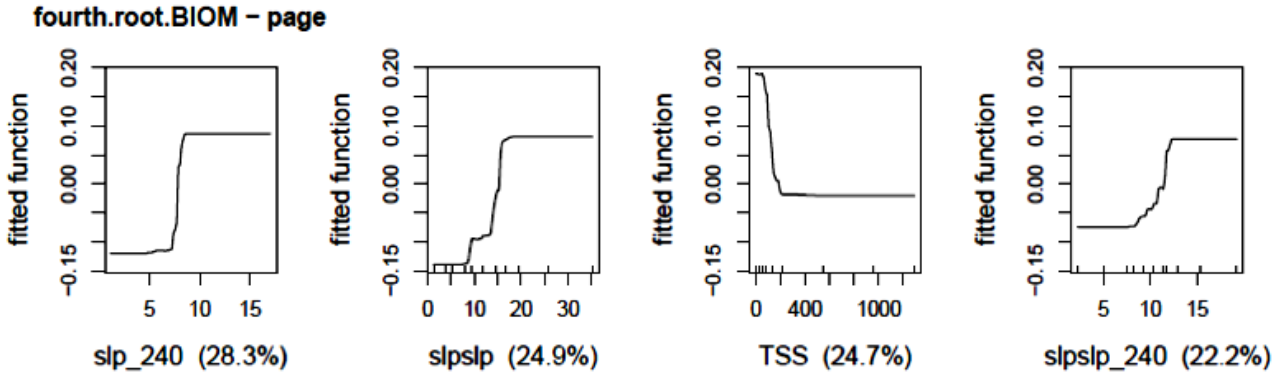


Fig S7. Response curves for total biomass. Curves show the relative relationships with selected terrestrial and marine drivers.

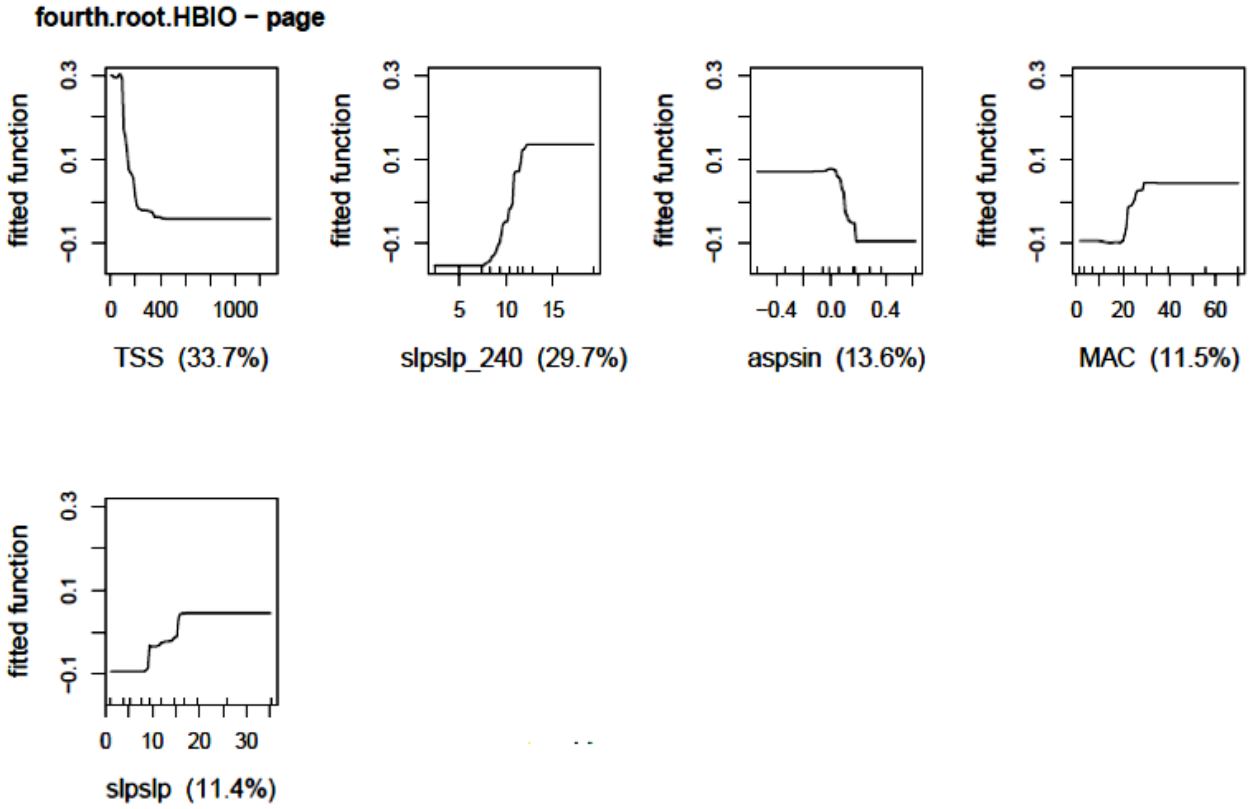


Fig S8. Response curves for herbivore biomass. Curves show the relative relationships with selected terrestrial and marine drivers.

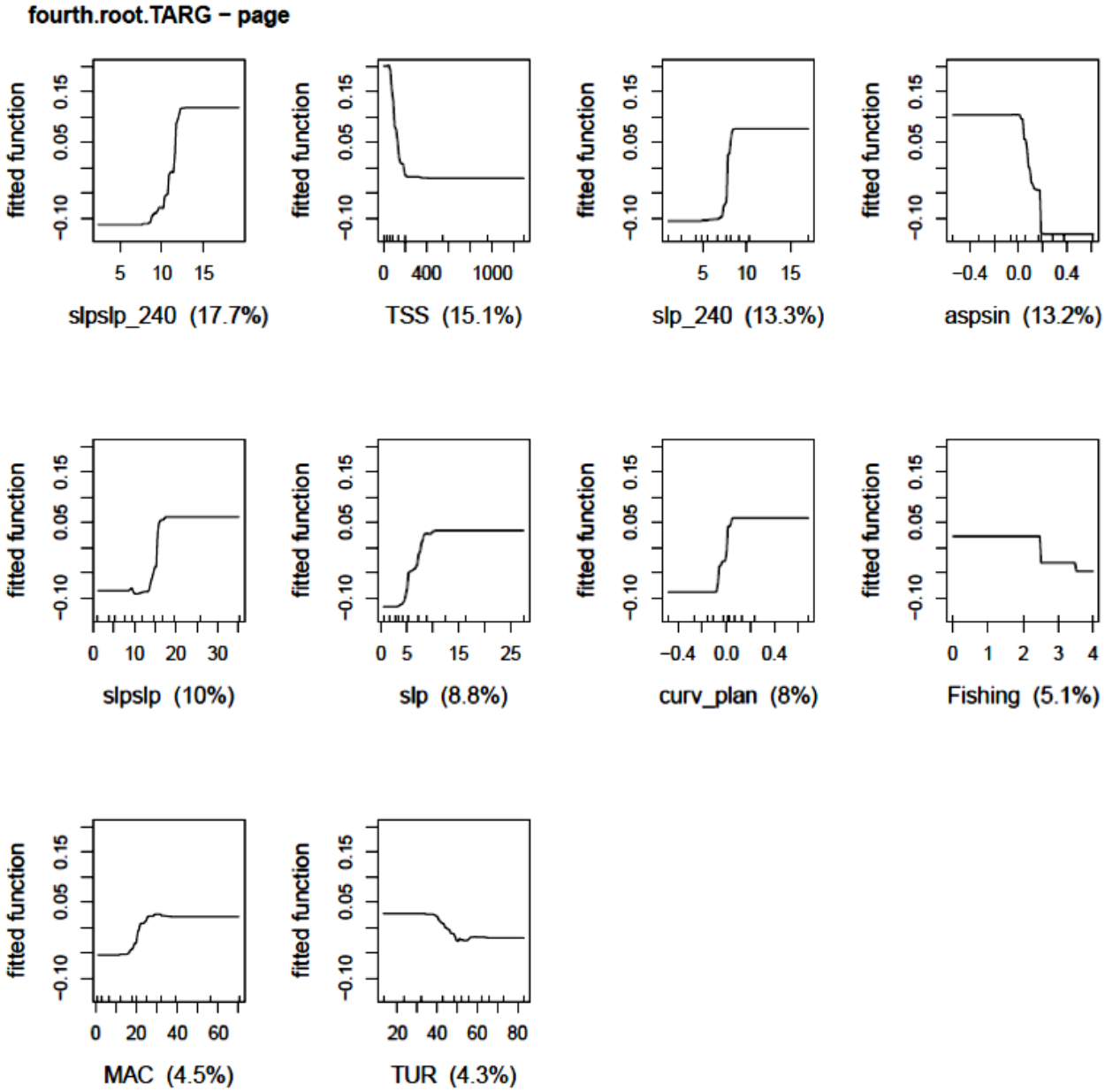


Fig S9. Response curves for targeted biomass. Curves show the relative relationships with selected terrestrial and marine drivers.

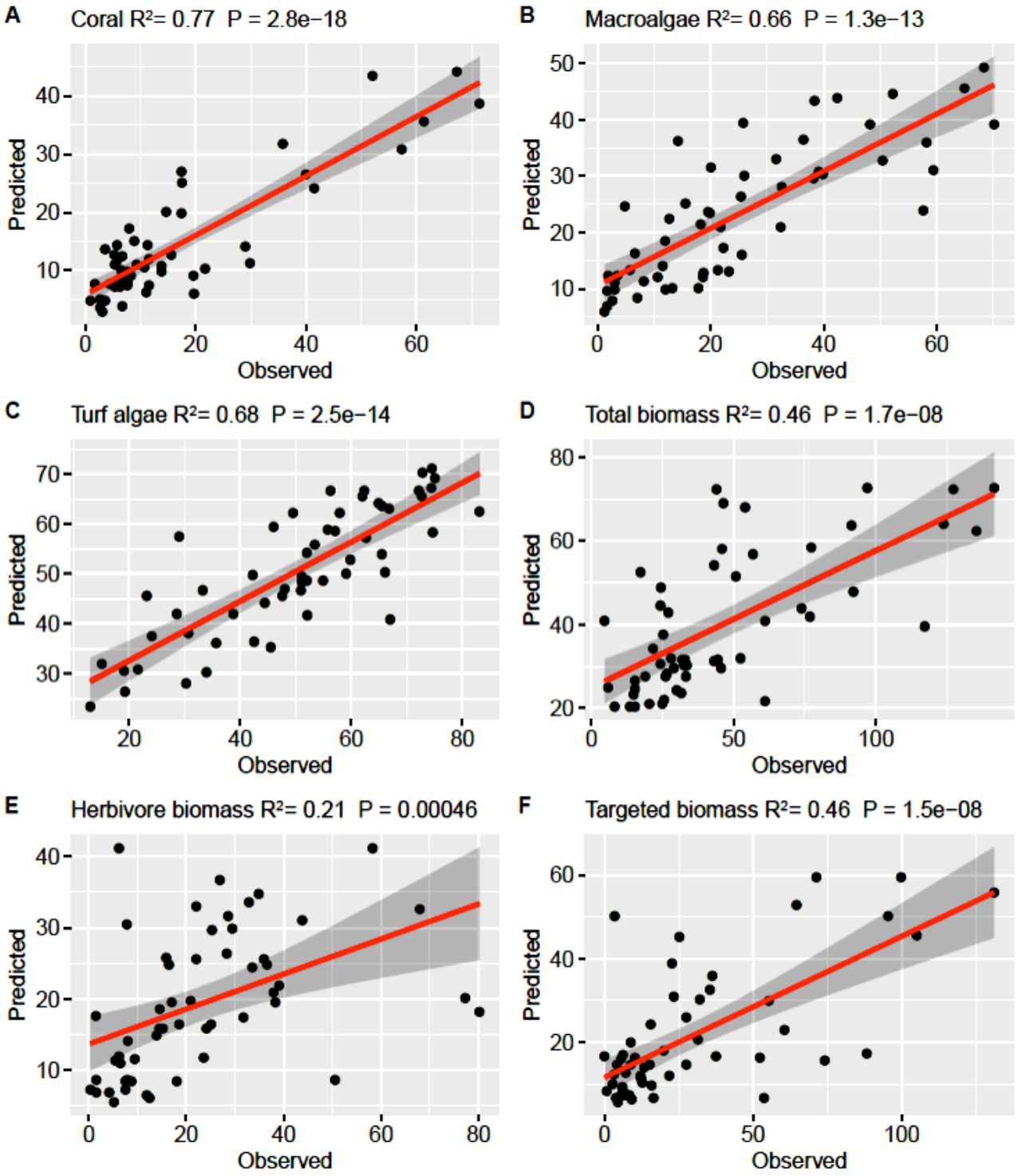


Fig S10. Coral reef indicators prediction validation

# APPENDIX 2 - TABLES

Table S1. Present land use/cover area ($km^2$ and %)

| Land use/cover | Area (ha) | % |
|---|---|---|
| Agriculture | 198.6 | 1.5 |
| Forest | 8946.4 | 69.1 |
| Golf course | 52.6 | 0.4 |
| Grassland | 1916.0 | 14.8 |
| Open land | 77.0 | 0.6 |
| Roads | 58.0 | 0.4 |
| Shrubland | 948.8 | 7.3 |
| Tree plantation | 34.2 | 0.3 |
| Settlement (L) | 377.9 | 2.9 |
| Settlement (M) | 254.1 | 2.0 |
| Settlement (H) | 84.2 | 0.7 |

**Table S2. Fish species recorded during marine surveys.** Fishes were identified to the lowest possible taxonomic level. Species considered as targeted by fishers are denoted by *. Herbivores are the 'Primary' consumer group.

| Scientific name | Family | Consumer group | Max size (cm) |
|---|---|---|---|
| *Abudefduf vaigiensis* | Damselfish | Planktivore | 20 |
| *Acanthurus blochii** | Surgeonfish | Primary | 43 |
| *Acanthurus dussumieri** | Surgeonfish | Primary | 56 |
| *Acanthurus lineatus** | Surgeonfish | Primary | 38 |
| *Acanthurus leucocheilus** | Surgeonfish | Primary | 45 |
| *Acanthurus nigrofuscus* | Surgeonfish | Primary | 23 |
| *Acanthurus olivaceus** | Surgeonfish | Primary | 40 |
| *Acanthurus pyroferus* | Surgeonfish | Primary | 25 |
| *Acanthurus* sp | Surgeonfish | Primary | 57 |
| *Acanthurus triostegus** | Surgeonfish | Primary | 27 |
| *Amphiprion* sp | Damselfish | Planktivore | 17 |
| *Anampses* sp | Wrasse | Secondary | 20 |
| *Anthias* sp | Anthias | Planktivore | 14 |
| *Anampses twistii* | Wrasse | Secondary | 18 |
| *Apogon* sp | Cardinalfish | Planktivore | 16 |
| *Aprion virescens** | Snapper | Piscivore | 112 |
| *Arothron nigropunctatus* | Pufferfish | Secondary | 33 |
| *Aulostomus chinensis* | Trumpetfish | Piscivore | 80 |

| Scientific name | Family | Consumer group | Max size (cm) |
|---|---|---|---|
| *Balistapus undulatus* | Triggerfish | Secondary | 30 |
| *Bodianus axillaris* | Wrasse | Secondary | 20 |
| *Bodianus loxozonus** | Wrasse | Secondary | 40 |
| Ostraciidae | Boxfish | Secondary | 41 |
| Chaetodontidae | Butterflyfish | Secondary | 25 |
| *Canthigaster amboinensis* | Pufferfish | Primary | 14 |
| *Canthigaster bennetti* | Pufferfish | Primary | 10 |
| *Calotomus carolinus** | Parrotfish | Primary | 54 |
| *Caranx melampygus** | Jack | Piscivore | 117 |
| *Cantherhines pardalis* | Filefish | Primary | 25 |
| *Caranx* sp* | Jack | Piscivore | 165 |
| *Caesio teres* | Fusilier | Planktivore | 40 |
| *Canthigaster valentini* | Pufferfish | Primary | 9 |
| *Centropyge bicolor* | Angelfish | Primary | 15 |
| *Centropyge bispinosa* | Angelfish | Primary | 10 |
| *Centropyge flavissima* | Angelfish | Primary | 14 |
| *Cetoscarus ocellatus** | Parrotfish | Primary | 90 |
| *Cephalopholis urodeta* | Grouper | Piscivore | 28 |
| *Chaetodon auriga* | Butterflyfish | Secondary | 23 |
| *Chaetodon baronessa* | Butterflyfish | Secondary | 16 |
| *Chlorurus bleekeri** | Parrotfish | Secondary | 49 |
| *Chaetodon citrinellus* | Butterflyfish | Secondary | 13 |
| *Cheilinus* sp | Wrasse | Secondary | 45 |
| *Chaetodon ephippium* | Butterflyfish | Secondary | 23 |
| *Cheilinus fasciatus* | Wrasse | Secondary | 36 |
| *Chaetodon kleinii* | Butterflyfish | Planktivore | 14 |
| *Chaetodon lineolatus** | Butterflyfish | Secondary | 30 |
| *Chaetodon lunulatus* | Butterflyfish | Secondary | 15 |
| *Chaetodon lunula* | Butterflyfish | Secondary | 21 |
| *Chlorurus microrhinos** | Parrotfish | Primary | 80 |
| *Chaetodon mertensii* | Butterflyfish | Primary | 13 |
| *Chaetodon pelewensis* | Butterflyfish | Secondary | 13 |
| *Chaetodon speculum* | Butterflyfish | Secondary | 18 |
| *Chlorurus sordidus** | Parrotfish | Primary | 40 |
| *Chaetodon trifascialis* | Butterflyfish | Secondary | 18 |
| *Chaetodon ulietensis* | Butterflyfish | Secondary | 15 |

| Scientific name | Family | Consumer group | Max size (cm) |
|---|---|---|---|
| *Chaetodon unimaculatus* | Butterflyfish | Secondary | 20 |
| *Chaetodon vagabundus* | Butterflyfish | Secondary | 23 |
| *Chlorurus* sp* | Parrotfish | Primary | 100 |
| *Coris gaimard* | Wrasse | Secondary | 40 |
| *Ctenochaetus binotatus* | Surgeonfish | Primary | 22 |
| *Ctenochaetus* sp | Surgeonfish | Primary | 30 |
| *Ctenochaetus striatus* | Surgeonfish | Primary | 28 |
| Herbivorous damselfish | Damselfish | Primary | 16 |
| Pomacentridae | Damselfish | Secondary | 17 |
| Planktivorous damselfish | Damselfish | Planktivore | 16 |
| *Epibulus insidiator* | Wrasse | Secondary | 54 |
| *Epinephelus merra** | Grouper | Piscivore | 33 |
| *Forcipiger flavissimus* | Butterflyfish | Secondary | 22 |
| Caesionidae | Fusilier | Planktivore | 31 |
| Mullidae* | Goatfish | Secondary | 50 |
| *Gomphosus varius* | Wrasse | Secondary | 32 |
| Serranidae* | Grouper | Piscivore | 128 |
| *Gymnothorax meleagris* | Moray | Piscivore | 120 |
| *Gymnosarda unicolor** | Tuna | Piscivore | 248 |
| *Gymnomuraena zebra* | Moray | Secondary | 150 |
| *Halichoeres hortulanus* | Wrasse | Secondary | 27 |
| *Heniochus chrysostomus* | Butterflyfish | Secondary | 18 |
| *Hemigymnus fasciatus* | Wrasse | Secondary | 50 |
| *Hemigymnus melapterus** | Wrasse | Secondary | 60 |
| *Heniochus monoceros* | Butterflyfish | Secondary | 23 |
| *Hemitaurichthys polylepis* | Butterflyfish | Planktivore | 18 |
| *Heniochus singularius* | Butterflyfish | Secondary | 30 |
| *Heniochus varius* | Butterflyfish | Secondary | 19 |
| *Hipposcarus longiceps** | Parrotfish | Primary | 60 |
| *Kyphosus cinerascens** | Chub | Primary | 51 |
| *Labroides bicolor* | Wrasse | Secondary | 14 |
| *Labroides dimidiatus* | Wrasse | Secondary | 12 |
| *Lethrinus* sp* | Emperor | Secondary | 86 |
| Synodontidae | Lizardfishes | Piscivore | 22 |
| *Lutjanus argentimaculatus** | Snapper | Secondary | 104 |
| *Lutjanus bohar** | Snapper | Piscivore | 90 |

| Scientific name | Family | Consumer group | Max size (cm) |
|---|---|---|---|
| *Lutjanus fulvus** | Snapper | Secondary | 40 |
| *Lutjanus gibbus** | Snapper | Secondary | 53 |
| *Lutjanus kasmira** | Snapper | Secondary | 40 |
| *Lutjanus monostigma** | Snapper | Piscivore | 60 |
| *Lutjanus semicinctus** | Snapper | Piscivore | 35 |
| *Macolor macularis** | Snapper | Planktivore | 60 |
| *Macolor niger** | Snapper | Planktivore | 75 |
| *Monotaxis grandoculis** | Emperor | Secondary | 63 |
| *Mulloidichthys flavolineatus** | Goatfish | Secondary | 40 |
| *Mulloidichthys vanicolensis** | Goatfish | Secondary | 38 |
| *Myripristis berndti** | Soldierfish | Planktivore | 33 |
| *Myripristis kuntee** | Soldierfish | Planktivore | 23 |
| Myripristinae* | Soldierfish | Planktivore | 35 |
| *Myripristis violacea** | Soldierfish | Secondary | 30 |
| *Naso hexacanthus** | Surgeonfish | Planktivore | 75 |
| *Naso lituratus** | Surgeonfish | Primary | 46 |
| *Naso unicornis** | Surgeonfish | Primary | 70 |
| *Naso vlamingii** | Surgeonfish | Planktivore | 60 |
| *Neoniphon sammara* | Soldierfish | Secondary | 32 |
| *Neoniphon* sp | Soldierfish | Secondary | 35 |
| *Oxycheilinus digramma* | Wrasse | Piscivore | 30 |
| *Oxymonacanthus longirostris* | Filefish | Secondary | 9 |
| *Oxycheilinus* sp | Wrasse | Secondary | 46 |
| *Paracirrhites arcatus* | Hawkfish | Secondary | 14 |
| *Parupeneus barberinus** | Goatfish | Secondary | 50 |
| *Parupeneus crassilabris** | Goatfish | Secondary | 35 |
| *Parupeneus cyclostomus** | Goatfish | Piscivore | 50 |
| *Paracirrhites forsteri* | Hawkfish | Piscivore | 23 |
| *Parupeneus multifasciatus** | Goatfish | Secondary | 38 |
| *Parupeneus pleurostigma** | Goatfish | Secondary | 33 |
| Scaridae* | Parrotfish | Primary | 68 |
| *Plectorhinchus picus** | Grunt | Secondary | 85 |
| *Pseudocheilinus octotaenia* | Wrasse | Secondary | 14 |
| *Ptereleotris evides* | Dartfish | Planktivore | 18 |
| *Pterois volitans* | Scorpionfish | Piscivore | 38 |
| *Pygoplites diacanthus* | Angelfish | Secondary | 25 |

| Scientific name | Family | Consumer group | Max size (cm) |
|---|---|---|---|
| Siganidae* | Rabbitfish | Primary | 38 |
| *Rhinecanthus aculeatus* | Triggerfish | Secondary | 30 |
| *Sargocentron caudimaculatum** | Soldierfish | Secondary | 25 |
| *Saurida gracilis* | Lizardfishes | Piscivore | 23 |
| *Sargocentron* sp* | Soldierfish | Secondary | 50 |
| *Sargocentron spiniferum** | Soldierfish | Secondary | 52 |
| *Scarus flavipectoralis** | Parrotfish | Secondary | 40 |
| *Scarus forsteni** | Parrotfish | Primary | 55 |
| *Scarus globiceps** | Parrotfish | Primary | 31 |
| *Scolopsis lineata* | Threadfin | Secondary | 20 |
| *Scarus niger** | Parrotfish | Primary | 43 |
| *Scolopsis* sp | Threadfin | Secondary | 20 |
| *Scarus psittacus** | Parrotfish | Primary | 33 |
| *Scarus rubroviolaceus** | Parrotfish | Primary | 70 |
| *Scarus schlegeli** | Parrotfish | Primary | 38 |
| *Scarus* sp* | Parrotfish | Primary | 130 |
| *Scarus tricolor** | Parrotfish | Primary | 55 |
| *Seriola dumerili** | Jack | Piscivore | 190 |
| *Siganus vulpinus* | Rabbitfish | Primary | 25 |
| *Parapercis* sp | Sandperch | Secondary | 23 |
| Holocentridae | Soldierfish | Secondary | 31 |
| *Stethojulis bandanensis* | Wrasse | Planktivore | 16 |
| *Sufflamen bursa* | Triggerfish | Secondary | 28 |
| *Sufflamen chrysopterum* | Triggerfish | Secondary | 22 |
| *Taeniura meyeni* | Stingray | Secondary | 180 |
| *Thalassoma hardwicke* | Wrasse | Planktivore | 20 |
| *Thalassoma jansenii* | Wrasse | Secondary | 20 |
| *Thalassoma lunare* | Wrasse | Planktivore | 25 |
| *Thalassoma lutescens* | Wrasse | Secondary | 25 |
| Labridae | Wrasse | Secondary | 93 |
| *Zanclus cornutus* | Moorish idol | Secondary | 20 |
| *Zebrasoma rostratum* | Surgeonfish | Primary | 21 |
| *Zebrasoma veliferum** | Surgeonfish | Primary | 40 |

Table S3. Terrestrial and marine drivers' description and processing methods

| Type | Code | Metric | Source | Description | Analytical tool |
|---|---|---|---|---|---|
| Terrestrial drivers | TSS | Total suspended sediment | InVEST SDR model | Proxy for total suspended sediment (t/yr) | Plume model |
| Marine geography | Depth | Depth | Bathymetry | Average depth (m) | ArcGIS Spatial Analyst tools (ESRI 2011) |
| Marine habitat topography | slp | Slope (30m, 240m) | Bathymetry | Maximum rate of change from a cell to its neighbors | ArcGIS Slope tool ArcGIS Focal Statistics tool (ESRI 2011) |
| Marine habitat exposure | asp | Surface aspect (mean) | Bathymetry | Slope direction (degrees) | ArcGIS Aspect tool (ESRI 2011) |
| | asp_sin | Sine aspect (30 m, 240 m) | Bathymetry | Sine of slope direction (derived from transforming the mean aspect into 'eastness') (degrees) | ArcGIS Spatial Analyst tools (sine function) (ESRI 2011b) |
| | asp_cos | Cosine aspect (30 m, 240 m) | Bathymetry | Cosine of slope direction (derived from transforming the mean aspect into 'northness') (degrees) | ArcGIS Spatial Analyst tools (cosine function) (ESRI 2011) |
| Marine habitat complexity | curv_prof | Profile curvature (mean) | Bathymetry | Curvature values can be + (concave), (convex), or 0 (flat). A proxy for spur and groove effects on water flow. | DEM Surface Tools Curvature tool (Jenness 2013) |
| | curv_plan | Planar curvature (mean) | Bathymetry | Curvature values can be – (concave) to + (convex), or 0 (flat) (mean). A proxy for spur and groove effects on water flow. | DEM Surface Tools Curvature tool (Jenness 2013) |
| Benthic community | COR | Coral cover | Coral reef model | Spatially explicit predicted % cover | Coral reef model predictions |
| | MAC | Macroalgae | Coral reef model | Spatially explicit predicted % cover | Coral reef model predictions |
| | TUR | Turf algae | Coral reef model | Spatially explicit predicted % cover | Coral reef model predictions |

This table provides a description of all the predictor variables modelled in the coral reef models. Each metric is classified by type (terrestrial drivers or marine drivers) and assigned a code for modelling.

**Table S4. Coral reef predictive model performance per indicator.** The percent deviance explained (PDE) by the BRT models for the calibration and cross-validation (CV) processes and the final number of drivers ($X_i$) is shown for Mele Bay.

| Indicators | PDE (%) | CV PDE (%) | CV SE (%) | Predictors (#) |
|---|---|---|---|---|
| Coral | 92.6 | 47.7 | 7.5 | 5 |
| Macroalgae | 86.6 | 29.0 | 13.8 | 8 |
| Turf algae | 77.9 | 42.1 | 7.9 | 6 |
| Total biomass | 44.6 | 22.0 | 18.7 | 4 |
| Herbivore biomass | 48.4 | 26.7 | 19.9 | 5 |
| Targeted biomass | 51.8 | 17.0 | 19.8 | 10 |

# APPENDIX 3 – LAND-SEA LINKED MODELLING FRAMEWORK METHODS

*from Delevaux et al. 2018*

## SEDIMENT MODEL – InVEST SDR

This approach relies on modelling sediment transport throughout the landscape based on local topography and therefore does not require hydrological modelling to determine the sediment ratio exported to the shoreline. The approach was initially proposed by Borselli et al. (2008) and has received increasing interest in recent years (Cavalli et al. 2013; López-Vicente et al. 2013).

First, we estimated the overland gross erosion per cell using the empirical Revised Universal Soil Loss Equation (RUSLE) (Renard et al. 1997) (see equation 1):

$$Soil\ loss = R \times K \times LS \times C \times P \qquad (1)$$

Where R = rainfall erosivity (MJ.mm.ha$^{-1}$.hr$^{-1}$), K = the rate of soil loss per rainfall erosion index unit, known as soil erodibility (ton-ha-hrs.MJ$^{-1}$ .ha$^{-1}$.mm$^{-1}$), LS = slope-length and gradient factor (derived from the DEM), C = a vegetation cover (C-factor), and P = management practice effectiveness (P-factor).

The SDR model is based on the concept of hydrological connectivity to estimate sediment retention and export to the shoreline (see Borselli et al. [2008] for more details). First, the SDR computes a connectivity index ($IC_i$) for each pixel i based on the upslope area and downslope flow path (Borselli et al. 2008). A streamflow accumulation threshold was set to define streams based on the DEM (Hamel et al. 2015b). Given the lack of empirical data for the region, the connectivity of the model was verified by comparing predicted stream outputs to available stream maps. Then, a sediment delivery ratio is derived for each pixel i based on the connectivity index (Hamel et al. 2015b). The SDR model parameters include an $IC_0$, a Borselli k-factor, and a maximum allowable SDR that define the shape of the relationship between the SDR and the connectivity index (Hamel et al. 2015b). The calibration parameters $IC_0$ and the k-factor were set to 0.5 and 2.0, respectively, and the maximum allowable SDR was set to 0.8 (Hamel et al. 2015b) (see Sharp et al. [2016] for more details on effects of parameterisation).

The sediment export per present and future scenario are reported at the sub-watershed and watershed scales. This approach was selected since it requires a minimal number of parameters and is spatially explicit. We note that the models have yet to be quantitatively validated against local datasets and were parameterised with values from other regions, which can differ in terms of climate and soil conditions (Gholami et al. 2009).

## Watershed delineation

Sub-watersheds were created by processing the DEM raster dataset (~ 30 x 30 m) of Efate, which was provided by the GEM division of SPC, with the ArcHydro toolset in ArcGIS, and pour points at the shoreline were edited for accuracy in comparison to satellite imagery and bathymetry data (DeVantier and Feldman 1993; Falinski 2016; Delevaux et al. 2018a). First, the sinks in the DEM were filled using the Fill Sinks tool so that any areas where water would get trapped had to be elevated to a point where that would no longer occur. Next, the flow path along the terrain was determined using the Flow Direction tool. Then, we calculated the number of grid cells that flow into any given cell in the DEM using the Flow Accumulation tool. At this point there was enough information to define streams within our study area.

A threshold of 1000 cells was chosen for the Stream Definition tool to define the stream network. Any cells that have a flow accumulation of 1000 or more would then be considered part of the stream network for our study area. The Stream Segmentation tool created a grid of stream segments that have a unique identification. From the output of the Stream Segmentation tool, we defined catchments using the Catchment Grid Delineation tool. There is essentially one catchment created for every stream segment. Next, a vector layer for streams was created using the Drainage Line Processing tool. Additionally, a vector layer for catchments was created using the Catchment Polygon Processing tool. Lastly, drainage points for each catchment were created using the Drainage Point Processing tool. These points represent tributaries and where they feed into larger streams, and eventually where river mouths let out into the ocean. The outputs were shapefiles representing the watersheds such that each watershed contributes to a discharge point (river mouth) where water quality will be analysed. The output stream map was compared to hydrographic maps of the Mele Bay study area.

## Rainfall erosivity index (R)

The rainfall-runoff erosivity factor (R) represents the erosion potential caused by rainfall. The rainfall-runoff erosivity factor is represented by a raster dataset with an erosivity index value for each cell. This variable depends on the intensity and duration of rainfall in the area of interest. It is defined as the long-term average of the product of total rainfall energy and the maximum 30-min intensity (I30) of rainstorms (Wischmeier and Smith 1978; Renard et al. 1997). The greater the intensity and duration of the rainstorm, the higher the erosion potential. Determining I30 requires at least 20 years of pluviograph data. Because the erosivity index is widely used, in case of its absence, there are methods and equations to help generate a grid using climatic data. [units: MJ.mm.(ha.h.yr)$^{-1}$]. Mean monthly precipitation data (1950–2000) were obtained from WorldClim's 30 arcsecond resolution Bioclim dataset (Fick and Hijmans 2017). The map of rainfall erosivity was derived from monthly rainfall averages at a 1 km x 1 km (P) and converted to erosivity using the Bols method applied in Indonesia (see equation 2):

$$R = \frac{2.5\ x\ P^2}{100(0.073P + 0.73)} \qquad (2)$$

# Soil erodibility (K)

Soil erodibility (K) is a measure of the susceptibility of soil particles to detachment and transport by rainfall and runoff. [units: tons.ha.h.(ha.MJ.mm)$^{-1}$]. K represents an integrated average annual value of the total soil and soil-profile reaction to many erosion and hydrologic processes. These processes include soil detachment and transport by raindrop impact and surface flow, localised deposition due to topography and tillage-induced roughness, and rainwater infiltration into the soil profile (Renard et al. 1997). K is defined as the rate of soil loss per erosivity index unit as measured on a standard plot 22.1 m long with a 9% slope, and continuously in a clean-tilled fallow condition, with tillage performed upslope and downslope (Renard et al. 1997). When profile permeability and structure are not available, soil erodibility can be estimated based on soil texture and organic matter content, based on the work of Wischmeier, Johnson and Cross (reported in Roose (1977).

K was derived from the World Inventory of Soil Emission Potentials (WISE) database (Batjes 2016). A special case is the K value for water bodies, for which soil maps may not indicate any soil type. A value of 0 can be used if no soil loss occurs in water bodies. We clipped the soil map to Efate and joined the table (Table: HW30s_MapUnit) from the global database to obtain the soil types for the island. The dataset included spatially categorised soil types based on similarities in soil characteristics. Each category contained information on percentage organic matter, the product of the primary particle size fraction, and the percentage of the top six abundant soil types. For this study, we focused on the topsoil and so we only needed to join with the topsoil Table PRID (HW30s_ParEst) from the global database.

K-factor was derived using equation 3 (Williams 1995) and the WISE derived soil properties on a 30 by 30 arc-seconds global grid (Batjes 2016).

$$K = f_{csand} \cdot f_{cl-si} \cdot f_{orgc} \cdot f_{hisand} \quad (3)$$

Where: $f_{csand}$ = a factor that gives low soil erodibility factors for soils with high coarse-sand contents and high values for soils with little sand, expressed in (ton/ha)*(ha.hr/MJ.mm) or t.ha.hr.(MJ.mm.ha)$^{-1}$, $f_{cl-si}$= a factor that gives low soil erodibility factors for soils with high clay to silt ratios, $f_{orgc}$ = a factor that reduces soil erodibility for soils with high organic carbon content, $f_{hisand}$ = a factor that reduces soil erodibility for soils with extremely high sand contents. The soil erodibility values (K) in this table are in US customary units and require the 0.1317 conversion (FAO 2007). The input factors of equation 3 are calculated with equations 4-7 below (Williams 1995);

$$f_{csand} = 0.2 + 0.3 \,.\, exp\,[-0.256 \,.\, ms \,.\, (1 - m_{silt}/100)] \quad (4)$$

$$f_{cl-si} = m_{silt}/(m_c + m_{silt})^{0.3} \quad (5)$$

$$f_{orgc} = 1 - (0.0256.\,\mathrm{orgC}\,/(\mathrm{orgC} + \exp\,[3.72 - 2.95.\,\mathrm{orgC}]) \quad (6)$$

$$f_{hisand} = 1 - (0.7.\,(1 - ms/100))/((1 - m_s/100) + exp(-5.51 + 22.9.\,(1 - m_s/100)) \quad (7)$$

Where: $m_s$ = % sand content, $m_{silt}$ = % silt content, $m_c$ = % clay content, orgC = % organic carbon. Soil erodibility is represented by a raster dataset, with a soil erodibility value for each cell (Fig S1).

## Land-use cover factors

The amount of protective coverage provided by the flora influences the soil erosion rate. Continuously fallowed and bare soils have a C value equal to 1. C values are lower when more vegetative coverage protects soils against erosion. Well-protected soils have a C value near 0. C-factors assigned to each land cover use/type in Vanuatu were derived from existing literature as estimated based on studies conducted in similar regions containing comparable land uses, from areas with similar geographic and physical processes, and consultation with experts (see Table 1 for more details on parameters) (Roose 1977; Wischmeier and Smith 1978; FAO 2007; Lianes et al. 2009; Doheny et al. 2013; Chicas and Omine 2015).

The Conservation Practice Factor (P) represents the impact of a specific conservation practice on soil erosion rates (Renard et al. 1997). It is the ratio of soil loss of a specific practice to the corresponding soil loss caused by up and down slope culture (Renard et al. 1997). Management practice effectiveness (P factor) was not considered in this model due to lack of data (Hamel et al. 2015b). Therefore, we assume the P value to be 1 throughout the entire region. Assigning C and P values to corresponding land uses was done by editing the attribute table of the land use shapefile in ArcGIS.

# WATER QUALITY MODEL

## Stream pour points

Pour points were created along with sub-watershed boundaries using the DEM (~ 30.7 x 30.7 m) of Vanuatu, provided by SPC GEM, with the ArcHydro toolset in ArcGIS. The pour point shapefile layer is the link between the terrestrial and marine models. The attribute table contains the watershed unique ID, the SDR results and the spatial feature point fall on the marine raster layers. The pour points at the shoreline were edited for accuracy in comparison to satellite imagery and available stream map (DeVantier and Feldman 1993; Delevaux et al. 2018a). Then the pour point shapefile was split into individual pour point shapefiles using the watershed unique ID to model individual total suspended sediment (TSS) plume (t/yr). Finally, the pour points were manually edited to align with the marine raster layers (e.g. bathymetry, currents).

## Decay plume model

We created a cost-path surface ($c$) that quantifies the least accumulative cost-distance (impedance) of moving planimetrically through each cell from each pour point using a composite of three marine drivers known to affect sediment dispersion: depth (m), distance to stream mouth (m) and current (degree and seconds) (Yu et al. 2003; Fabricius 2005a; Delevaux et al. 2018a) (see 'Cost distance raster' section below for more details). Then, the spread of sediment into coastal waters from each pour point was modelled using a decay function, which assigned a portion of the remaining quantity from the previous cell in all adjacent cells based on the cost-path surface until a maximum distance of 3 km from the shoreline was reached (Halpern et al. 2008; Delevaux et al. 2018a) (see equation 8). This threshold was based on distance measured in ArcGIS between river mouths

$$S_i = s_p \times e^{-c^2/D_c} \quad (8)$$

where $S_i$ = grid cell value for dispersed sediment (t. $yr^{-1}$) for watershed i, $S_P$ = sediment ($m^3.yr^{-1}$) load (t. $yr^{-1}$) at each watershed pour point (obtained from summarizing the total sediment export per watershed), $c$ = cost-path surface (unitless), $D_c$ = cost-path surface threshold distance from the shore for each decayed sediment plume per watershed (equivalent to 3 km from the shoreline). Last, we summed all the individual watershed sediment plume gridded maps in ArcGIS to obtain the total suspended sediment (represented by TSS) per land-use scenario for each pixel of coral reef area. This approach to modelling coastal sediment discharge is diffusive and thus allows for wrap-around coastal features, but does not account for nearshore advection that acts to push suspended sediment in specific directions (Halpern et al. 2008). We used these diffusive models to derive conservative estimates of sediment plumes since the nearshore circulation patterns were unknown for our study site.

## Distance cost raster

A distance cost raster, which accounts for the cost of depth and current forcing on each grid cell, was generated for each watershed using the cost allocation tool for each pour point and a total cost raster dataset in ArcGIS. The total cost raster layer was generated by summing the current and depth cost layers for each watershed in R. The current and depth cost layers were derived from the current and bathymetry data using the methods described below.

## Current cost layers

First, we determined the travel time layer from each pour point due to the current data. To determine how surface currents could affect the lateral movement of sediment we used the Path Distance tool in ArcGIS (Doheny et al. 2013; Rude et al. 2016). The path distance tool creates an output raster in which each cell is assigned the accumulative cost from the cheapest source cell while accounting for surface distance, and horizontal and vertical cost factors. The algorithm utilises a node/link cell representation. The cost to travel between one node and the next depends on the spatial orientation of the nodes. How the cells are connected impacts the travel cost as well. Every link has a specific impedance associated with it, which is derived from the costs associated with the cells at each end of the link (from the cost raster) as well as the direction of movement. This tool requires: 1) a source (i.e. the individual river mouth pour points shapefiles); 2) cost raster (seconds); 3) input horizontal raster (degree); and 4) a horizontal factor.

The horizontal factor is a user-specified parameter required for the path distance tool that defines the relationship between the horizontal cost factor (seconds to cross each cell) and the horizontal relative moving angle. The horizontal factor defines the horizontal difficulty encountered when moving from one cell to the next (ESRI 2011a). The horizontal relative moving angle identifies the angle between the horizontal direction of a cell and the moving direction (ESRI 2011a). For the horizontal factor, we had no additional data other than the Hybrid Coordinate Ocean Model (HYCOM) average monthly surface currents, therefore we had no information to tell us that sediment would go anywhere other than 'downstream'. To address this, we chose to use the 'forward' pre-set parameter setting which establishes that only forward movement is allowed (i.e. down current). The result of this model was an accumulated cost in seconds to travel towards or away from each river mouth in our study region while accounting for surface current forcing.

The input cost raster and the horizontal raster were both derived from HYCOM surface current data. To determine mean monthly ocean currents around Vanuatu, we also used HYCOM (HYCOM 2013). HYCOM models are isopycnal (constant potential density) in the open, stratified ocean, which is the only regional data that were available to us for this study. The spatial resolution of the data is 1/12°

(~9 km). To acquire the HYCOM data we used the get.hycom function from the HMMoce package (Braun et al. 2018) in R to download 10 years of HYCOM surface current data (1993–2002) to overlap with the precipitation data used for the SDR modelling (1950–2000). For this study, we used the mean yearly east-west (u) and north-south (v) velocity components of the surface currents. R package ncdf4 (Pierce 2019) was used to manipulate the netcdf files and store the extracted data in a three-dimensional array. Arrays were converted to raster bricks and current data were averaged by month and then by year using the raster package in R (Hijmans 2019).

Finally, current data was averaged for the entire 10-year period for u and v variables and output as rasters. The datasets were clipped for Vanuatu coastline and converted to a point shapefile in ArcGIS. The nearshore gaps were filled using the Inverse Distance Weighting interpolation tool in ArcGIS and converted to 100 m x 100 m resolution rasters. To create the seconds and degree layers, we used Raster Calculator to derive the time in seconds (cost) that it would take to cross an individual cell. To do this we took the width of each pixel (100 m) and divided it by the resulting velocity of the two interpolated annual monthly averaged u (E-W) and v (N-S) vectors (in m $s^{-1}$) derived from HYCOM data (1993–2002) (Doheny et al. 2013) (see equation 9):

$$Seconds = \frac{Distance\ across\ the\ cell}{\sqrt{(u^2) + (v^2)}} \quad (9)$$

For the horizontal raster we needed to determine the direction the resulting vector was going across each cell. We did this by taking our u and v velocities and determining an angle of movement. To determine this angle for each pixel we used the following function in Raster Calculator:

$$Degree = (|\,\mathrm{ATan2}(u, v) * \frac{180}{\pi}| - 180) \quad (10)$$

Lastly, we determined the travel time cost from each pour point due to the current data. The accumulated cost, in seconds to travel towards or away from each river mouth in our study region while accounting for surface current forcing, was reclassified into 20 bins based on quantiles. The output is a current cost layer, which assumes that the diffusion cost increases with distance from the stream mouth (Delevaux et al. 2018a).

## Bathymetry cost layers

The bathymetry layer used for this study is the General Bathymetric Chart of Oceans (GEBCO) (~500 m x 500 m) and was downloaded from https://www.gebco.net/ for the area of interest (Weatherall et al. 2015). The dataset was converted to a point shapefile and the nearshore gaps were filled using the Inverse Distance Weighting interpolation tool in ArcGIS. The final bathymetry raster dataset used for this analysis was 100 m x 100 m. In R, the bathymetry layer was reclassified into 20 bins based on quantiles. The output is a depth cost layer, which assumes that diffusion cost is higher in shallower waters (Delevaux et al. 2018a).

# APPENDIX 4 – DATA GAPS AND CAVEATS

## *Adapted from Delevaux et al. 2018*

This decision-support tool was developed and implemented in a data-poor region and therefore under several key data gaps and caveats. First, the resolution of the input foundational layers, including the soils (~900 m x 900 m), rainfall (~900 m x 900 m), and currents (9 km x 9 km) are coarse resolution for the four watersheds discharging into Mele Bay. Because soil and rainfall maps are coarser resolution than the DEM input at which SDR operates, it may obscure small scale processes and spatial nuances, which can occur in small watersheds and narrow reef systems often found in tropical oceanic island environments (Delevaux et al. 2019). In addition to the low resolution, the sediment export loads may be underestimated due to erosion processes not accounted for in our modelling approach, such as land slip and stream bank erosion, which can be major sources of sediment (Olley et al. 2015; Brown et al. 2017a). It is also important to note that the current maps were interpolated nearshore to fill in the gaps along the shoreline, which may create erroneous values. This may have impacted the dispersion of the TSS plume in the study area. In addition, no in situ water quality data was available for the streams and coastal waters modelled, which prevented us from ground-truthing the sediment and coastal plume models.

However, we manually digitised the land use/land cover map using recent satellite imagery to ensure accuracy and a high-resolution LiDAR bathymetry layer (5m x 5m) was available for the whole study area, which helped refined the plume dispersion model and provide input layers for species distribution modelling. Future work should investigate how these modelled plumes of TSS compare to local knowledge from coastal communities, satellite imagery, and/or in situ data as those become available. In the meantime, spatial planning requires information to prioritise efforts on the ground and these global datasets are freely available for data-poor regions such as Vanuatu.

Our models were calibrated on contemporary conditions using empirical data collected in November 2019. Based on a number of assumptions, they can be used to forecast biological indicator distributions at a different point in time (Franklin 2010). A key assumption with predicting coral reef futures in our modelling approach is that species distributions are in equilibrium with current conditions and the identified relationships will remain constant over time (DeAngelis and Waterhouse 1987; Franklin 2010), which may not always be true (Carpenter 2002). While our sediment models accounted for the connectivity across the landscape (Hamel et al. 2015b), the marine models do not account for species dispersal, migration or interactions within the seascape, which can influence management scale and outcomes (Guisan 2005; Stamoulis and Delevaux 2015).

Given imperfect knowledge of both the effects of human drivers and how coral reefs respond to these drivers (Coreau et al. 2009), scenario modelling requires simplifications and assumptions, which lead to uncertainty in model projections (Delevaux et al. 2018a). By using present conditions as the baseline for examining projected coral reefs, the comparative benchmark represents potentially impacted ecosystems (Knowlton and Jackson 2008). Nevertheless, while sources of uncertainty in scenario analysis are inevitable, present conditions still provide an opportunity to identify the trajectory of coral reefs under different human drivers and provide guidance for management (Alagona et al. 2012). We used scenario modelling to illustrate the range of possibilities for the future of coral reefs and test local management actions that can reduce the risk of impacts on coral reefs and associated marine resources (Coreau et al. 2009).

Another key assumption associated with predicting futures with static models is that the effects of time lags and the complex, nonlinear relationships between land-use practices and coral reef benefits are not accounted for, which can influence management scale and outcomes (Toonen et al. 2011). For

instance, the restoration and urbanisation scenarios assumed restoration and clearing was immediate. In reality, restoration is not an instantaneous process as it will take many years before a forest is established enough to provide the sediment retention and runoff reduction we considered; therefore, sediment export would differ from the total export modelled here. Similarly, clearing proceeds in a patchwork over time and different areas would have different amounts of ground cover or regrowth at different times (Tulloch et al. 2016). From a marine perspective, coral reef response to change in sediment runoff and water will also vary over time based on taxon physiology and environmental conditions (Anthony 2006b). Thus, from a management perspective, it is essential to account for the timeframe of anticipated outcomes of conservation actions to factor in social and economic constraints (Saunders et al. 2017).

This research identified where coral reef areas may be subject to sediment exposure but did not explicitly model potential interactions with nutrients or climate change and cumulative impacts due to a lack of data and the poor understanding of those processes (Anthony 2006a; Wenger et al. 2015; Morgan et al. 2016). It is increasingly recognised that water quality in combination with elevated sea surface temperature (SST) can have a profound influence on management outcomes of nearshore coral reefs under climate change (Anthony et al. 2007). Recent work has shown that sediments can have an antagonistic effect with SST by mitigating bleaching impacts through shading (Anthony 2006a; Anthony et al. 2007), while other research has shown that excess nutrients or fishing pressure can prevent recovery from climate change impacts (Wooldridge 2009b; Wilson et al. 2010).

Finally, this study focused on the impact of sediment runoff due to land cover change on coral reefs. It did not consider seagrass and mangrove habitats, which are vulnerable to sediment runoff and provide important ecosystem goods and services. Seagrass meadows and mangroves serve as nursery habitats for a number of fishery species (Nagelkerken et al. 2000). Seagrass meadows also serve as critical feeding areas for dugongs and sea turtles (Sheppard et al. 2007), and mangroves trap sediments, prevent coastal erosion and protect coastlines from natural disasters (Marois and Mitsch 2015). Furthermore, seagrass and mangrove systems act as significant carbon sinks, thus mitigating global climate change (Duarte et al. 2013). Previous research has shown that sedimentation can reduce seagrass habitat suitability (Saunders et al. 2017). The relationship between sediment loads and seagrass-suitable habitat is non-linear, with large increases in sediment disproportionately impacting the availability of seagrass-suitable habitat. Similarly, it is shown in over 26 cases around the world that excess sediment inputs to mangroves can cause death of trees owing to root smothering, even if mangroves flourish on sedimentary shorelines (Ellison 1999). However, there are insufficient data to establish specific tolerances. Quantifying the links between sediment exports and impacts to coastal habitats is required to calculate the trade-offs of conservation actions on land in terms of benefits accrued in the ocean. Therefore, spatially explicit decision-support tools that capture the impact of land-based source pollution on those ecosystems must be the focus of future research and development, while mangroves and seagrass beds remain to be mapped in Vanuatu.

**Produced by the Pacific Community (SPC)**
Suva Regional Office,
Private Mail Bag,
Suva, Fiji
+ 679 337 0733
spc@spc.int | spc.int



ISBN 978-982-00-1390-2